

Lagrangian Dispersion in Gaussian Self-Similar Velocity Ensembles

Marta Chaves,¹ Krzysztof Gawędzki,^{2,5} Peter Horvai,^{2,3} Antti Kupiainen,⁴ and Massimo Vergassola^{1,5}

Received March 17, 2003; accepted July 10, 2003

We analyze the Lagrangian flow in a family of simple Gaussian scale-invariant velocity ensembles that exhibit both spatial roughness and temporal correlations. We argue that the behavior of the Lagrangian dispersion of pairs of fluid particles in such models is determined by the scale dependence of the ratio between the correlation time of velocity differences and the eddy turnover time. For a non-trivial scale dependence, the asymptotic regimes of the dispersion at small and large scales are described by the models with either rapidly decorrelating or frozen velocities. In contrast to the decorrelated case, known as the Kraichnan model and exhibiting Lagrangian flows with deterministic or stochastic trajectories, fast separating or trapped together, the frozen model is poorly understood. We examine the pair dispersion behavior in its simplest, one-dimensional version, reinforcing analytic arguments by numerical analysis. The collected information about the pair dispersion statistics in the limiting models allows to partially predict the extent of different phases of the Lagrangian flow in the model with time-correlated velocities.

KEY WORDS: Turbulence; Lagrangian flow; scaling.

1. INTRODUCTION

The aim of this paper is to study the Lagrangian flow in d -dimensional random velocity fields $\mathbf{v}(t, \mathbf{r})$ with a prescribed scale-invariant statistics. The velocity ensembles that we shall consider mimic some essential properties of

¹ Observatoire de la Côte d'Azur, B.P. 4229, 06304 Nice, France.

² Laboratoire de Physique, ENS-Lyon, 46 Allée d'Italie, 69364 Lyon, France; e-mail: kgawedsk@ens-lyon.fr

³ Centre de Physique Théorique, École Polytechnique, 91128 Palaiseau, France.

⁴ Department of Mathematics, Helsinki University, P.O. Box 4, 00014 Helsinki, Finland.

⁵ Member of CNRS.

realistic velocities in developed turbulence: their spatial roughness within a large interval of scales and their temporal correlation. By definition, the Lagrangian flow is described by the ordinary differential equation

$$\frac{d\mathbf{R}}{dt} = \mathbf{v}(t, \mathbf{R}). \quad (1.1)$$

It determines the motion of hypothetical fluid particles or of small test particles suspended in the fluid. One usually distinguishes between the motion of a single particle, dominated by the velocity fluctuations on the largest scale present (the so called “sweeping effects”) and the evolution of a relative separation of two particles. The latter is driven by the velocity fluctuations on scales of the order of the inter-particle distance and it is the main object of interest of the present paper. For larger groups of particles, one should similarly distinguish the motion of their barycenter from the relative motion of particles within the group. The latter is known to show quite intricate behavior related to intermittency, see ref. 14, but it will not be discussed here.

The separation $\boldsymbol{\rho} = \mathbf{R}' - \mathbf{R}$ between two fluid particles satisfies the equation

$$\frac{d\boldsymbol{\rho}}{dt} = \mathbf{v}(t, \boldsymbol{\rho} + \mathbf{R}(t)) - \mathbf{v}(t, \mathbf{R}(t)), \quad (1.2)$$

where $\mathbf{R}(t)$ is a trajectory of one of the particles, a solution of Eq. (1.1) starting at time zero at $\mathbf{R} = 0$, for example. Upon introduction of the so called quasi-Lagrangian velocity,

$$\mathbf{v}^{qL}(t, \mathbf{r}) = \mathbf{v}(t, \mathbf{r} + \mathbf{R}(t)), \quad (1.3)$$

i.e., velocity in the frame moving with a fixed fluid particle, we may rewrite Eq. (1.2) as

$$\frac{d\boldsymbol{\rho}}{dt} = \mathbf{v}^{qL}(t, \boldsymbol{\rho}) - \mathbf{v}^{qL}(t, \mathbf{0}) \equiv \Delta \mathbf{v}^{qL}(t, \boldsymbol{\rho}). \quad (1.4)$$

We shall be interested in the short- and long-time behaviors of the Lagrangian particles in the statistical ensembles where typical velocities are only Hölder continuous, the property expected in the limit of infinite Reynolds numbers.⁽³²⁾ In such non-Lipschitz velocities, there is a problem with solving Eqs. (1.1), (1.2), or (1.4). To avoid it, we shall first consider noisy particle trajectories that solve the stochastic equation

$$d\mathbf{R} = \mathbf{v}(t, \mathbf{R}) dt + \sqrt{2\kappa} d\mathbf{W}, \quad (1.5)$$

where $\mathbf{W}(t)$ is the Brownian motion in d dimensions mimicking the effect of molecular diffusivity. Noisy trajectories form a well defined Markov process even in velocity fields with poor regularity. Subsequently, the limit $\kappa \rightarrow 0$ will be performed in selected quantities. Other regularizations may be considered.^(12, 13) For example, the velocity field may be smeared at short distances to mimic the effects of viscosity, the trajectory equations solved in smeared velocities and the smearing removed subsequently. Such a procedure may lead to a different limiting flow, see remarks at the end of Section 2. For definiteness, we shall consider in the present paper only the Lagrangian flows defined with the use of the Brownian noise regularization. Physically, this corresponds to the small Prandtl number situations where on small scales the molecular diffusion masks the viscous effects. The simple velocity ensembles that we shall discuss are time-reversal invariant. As a result, we shall not have to distinguish the forward and the backward evolution of trajectories and will concentrate on the first one, between, say, times zero and t .

One way to study the relative motion of pairs of fluid particles is to follow the evolution of the **pair dispersion**, i.e., of the separation distance ρ between two particles. Its statistics in a random flow may be described by the velocity-averaged probability distribution $\mathcal{P}(t, \rho_0; d\rho)$ of the time t dispersion ρ , given its time zero value ρ_0 , in the limit when we remove the (independent) noises of the Lagrangian trajectories. Another, related, test of the relative motion of a pair of fluid particles is obtained by looking at the **exit time**:^(21, 6) the time t that the pair dispersion takes to evolve from ρ_0 to ρ_1 . In particular, $\rho_1 = 2\rho_0$ corresponds to the **doubling time** of the pair dispersion. The statistics of the exit times may be encoded in their velocity-averaged distribution $\mathcal{Q}(\rho_0, \rho_1; dt)$ taken in the limit of vanishing noise. Unlike $\mathcal{P}(t, \rho_0; d\rho)$, the distribution $\mathcal{Q}(\rho_0, \rho_1; dt)$ may integrate to less than 1 with the missing mass determining the probability of the events when the pair dispersion does not attain the value ρ_1 in finite time. The exit time is less influenced than the pair dispersion by small or large-distance cutoffs in the velocity correlations, so preferable in numerical or experimental studies.⁽⁶⁾

Recently, a new insight into the intricate character of the Lagrangian flow in turbulent velocities has been gained by analytic study of the Kraichnan ensemble⁽²⁷⁾ of Gaussian velocities which are decorrelated in time but exhibit scaling behavior in space, see refs. 5, 12, 23, 28, and 29. Here, we try to find out how the presence of temporal correlations of velocities influences the Lagrangian flow. We shall study the behavior of trajectory separation in a simple generalization of the Kraichnan ensemble of velocities where time correlations are reintroduced.

The paper is organized as follows. In Section 2 we recall the main facts about the Lagrangian flow in the Kraichnan model, in particular the

appearance of phases with very different trajectory behavior. Section 3 describes a Gaussian ensemble of homogeneous isotropic velocities with temporal correlations, discussed in the past in refs. 2, 10, 15, and 18 and similar in the spirit to non-isotropic shearing ensembles studied in refs. 3 and 4, see also ref. 30. We present a simple mean-field type analysis of the particle separation when such an ensemble is used to model the quasi-Lagrangian velocities. How the mean-field predictions may be substantiated further by scaling arguments is the subject of Section 4. See also refs. 16 and 17 for related rigorous results. Analytic arguments and conjectures about the behavior of trajectories in a one-dimensional version of the model with time-independent velocities are contained in Section 5. The simple geometry of this case allows for an analytic treatment. The behavior of the exit time statistics in velocity ensembles with long-time correlations is briefly studied in Section 6. The question how the behavior of pair dispersion changes when the Gaussian ensemble is used to model the Eulerian velocities is addressed in Section 7. In particular we show that in the one-dimensional time-independent case, the sweeping by large eddies in the Eulerian model speeds up the movement of a single Lagrangian particle, but it localizes pairs of particles by reducing the growth of their dispersion. Five Appendices contain more technical material. Some of the predictions of the paper are checked in one dimension by numerical simulations.

2. LESSONS FROM THE KRAICHNAN MODEL

The **Kraichnan ensemble** of turbulent velocities,⁽²⁷⁾ is a Gaussian ensemble with vanishing velocity 1-point function and with the 2-point function

$$\langle v^i(t, \mathbf{r}) v^j(t', \mathbf{r}') \rangle = D_1 \delta(t-t') \int \frac{e^{i\mathbf{k} \cdot (\mathbf{r}-\mathbf{r}')}}{k_L^{d+\xi}} P^{ij}(\mathbf{k}, \wp) \frac{d\mathbf{k}}{(2\pi)^d}, \quad (2.1)$$

where $k_L = \sqrt{k^2 + L^{-2}}$ and $P^{ij}(\mathbf{k}, \wp) = \frac{1-\wp}{d-1} (\delta^{ij} - \frac{k^i k^j}{k^2}) + \wp \frac{k^i k^j}{k^2}$, see ref. 14 and references therein. There are two dimensionless parameters in the Kraichnan ensemble: the exponent $\xi > 0$ and the compressibility degree $0 \leq \wp \leq 1$. For $\xi \leq 2$, the velocities smeared in time are (almost surely) Hölder continuous in space with any exponent smaller than $\xi/2$. For $\xi > 2$, they are Lipschitz (or even more regular). The compressibility degree $\wp = 0$ corresponds to incompressible velocities, $\wp = 1$ to gradients of a potential (in one dimension necessarily $\wp = 1$). The normalization constant D_1 has dimension $length^{2-\xi}/time$. The length L is the integral scale that sets the spatial correlation length of velocities. If $\xi < 2$, it may be taken to infinity in the

correlation functions involving only velocity differences $\mathbf{v}(t, \mathbf{r} + \boldsymbol{\rho}) - \mathbf{v}(t, \mathbf{r}) \equiv \Delta \mathbf{v}(t, \boldsymbol{\rho})$. For $\xi = 2$, this may still be done if D_1 is rescaled when $L \rightarrow \infty$.

2.1. Possible Flow Behaviors

The Kraichnan ensemble may be used invariably to model Eulerian or quasi-Lagrangian velocities as both ensembles coincide in this case. The statistics of a single Lagrangian particle is that of a d -dimensional Brownian motion with diffusivity that blows up when $L \rightarrow \infty$. The two-particle separation depends only on velocity differences and its statistics has a non-trivial $L \rightarrow \infty$ limit whenever this holds for the velocity differences. The pair-dispersion and the exit time distributions $\mathcal{P}(t, \rho_0; d\rho)$ and $\mathcal{Q}(\rho_0, \rho_1; dt)$ may be solved analytically in this limit. The exact solutions, that describes also the short-distance asymptotics of the distributions at finite L , show several dichotomic behaviors depending on the values of parameters of the model. The first dichotomy, noticed in ref. 5, is between the

deterministic flow characterized by the property

$$\lim_{\rho_0 \rightarrow 0} \mathcal{P}(t, \rho_0; d\rho) = \delta(\rho) d\rho \quad (2.2)$$

which signals that the trajectories in a fixed velocity field are defined by their initial position, and the

stochastic flow where

$$\lim_{\rho_0 \rightarrow 0} \mathcal{P}(t, \rho_0; d\rho) \text{ is a measure with density.} \quad (2.3)$$

The limits of the probability distributions above (and below) should be understood in weak sense, under integrals against test functions. The behavior (2.3) means that infinitesimally close trajectories separate in a finite time and indicates that the stochasticity introduced into the Lagrangian flow by coupling it to the noise, see Eq. (1.5), survives in the limit $\kappa \rightarrow 0$. The Lagrangian trajectories in a fixed velocity field are not determined by initial position but form instead a stochastic process. That this is indeed what happens in the Kraichnan model was established rigorously in ref. 28. We shall call the phenomenon **spontaneous stochasticity**.⁶

There are further dichotomic behaviors of the Lagrangian flow in the Kraichnan model. We have chosen to characterize the other dichotomies in terms of the small ρ_0 behavior of the exit time distribution $\mathcal{Q}(\rho_0, \gamma\rho_0; dt)$

⁶ It was termed intrinsic stochasticity in ref. 12.

with $\gamma \neq 1$ fixed, attaching to them more or less suggestive names. There is a dichotomy between the

Lyapunov flow such that

$$\lim_{\rho_0 \rightarrow 0} \mathcal{Q}(\rho_0, \gamma\rho_0; dt) \text{ is a measure with density,} \quad (2.4)$$

and the

Richardson flow where

$$\lim_{\rho_0 \rightarrow 0} \mathcal{Q}(\rho_0, \gamma\rho_0; dt) = c(\gamma) \delta(t) dt \quad \text{with } c(\gamma) > 0. \quad (2.5)$$

This dichotomy distinguishes the flows in regular velocities where the Lagrangian separation on short distances involves fixed time scales (like the inverse Lyapunov exponent), from the ones in non-regular (non-Lipschitz) velocities where the characteristic times of the Lagrangian separation become very short on short scales.

Finally, the last two dichotomies that we want to single out characterize the short distance behavior of the probability of infinite exit times. They are between the

locally separating and locally trapping flow where for $\gamma > 1$

$$\lim_{\rho_0 \rightarrow 0} \int \mathcal{Q}(\rho_0, \gamma\rho_0; dt) \left\{ \begin{array}{l} = \\ < \end{array} \right\} 1, \text{ respectively,} \quad (2.6)$$

and

locally recurrent and locally transient flow where the same holds for $\gamma < 1$.

Roughly, with positive probability, close trajectories do not increase their distance in locally trapping flows and do not approach each other in locally transient ones.

2.2. Pair Dispersion

Due to the temporal decorrelation of the Kraichnan velocities, the probability distributions $\mathcal{P}(t, \rho_0; d\rho)$ constitute transition probabilities of a Markov process $\rho(t)$ that in the limit $L \rightarrow \infty$ becomes a diffusion on a half-line with the explicit generator

$$M = -D'_1 \rho^{\xi-a} \partial_\rho \rho^a \partial_\rho \quad \text{for } a = \frac{d+\xi}{1+\wp\xi} - 1, \quad (2.7)$$

where D'_1 is proportional to D_1 . Note that the symbol of M vanishes at $\rho = 0$. The different behavior of such diffusion for different values of ξ and a has its origin in the singularity of M at $\rho = 0$ which requires different treatment in different regimes. Up to the change of variables $x = \rho^{(2-\xi)/2}$ casting the generator M into the form

$$M = \left(1 - \frac{\xi}{2}\right)^2 D' x^{1-\delta} \partial_x x^{\delta-1} \partial_x \quad \text{for} \quad \delta = 2 \left(1 - \frac{1-a}{2-\xi}\right) \quad (2.8)$$

and a time rescaling, the Markov process $\rho(t)$ may be identified with the well studied Bessel diffusion,⁽⁷⁾ a natural interpolation between processes describing the radial variable in the standard diffusion in integer dimensions δ . Various analytic formulae may be then directly carried from that case to the present situation.

For $\xi = 2$ corresponding to smooth velocities with velocity differences linear in space, the particle dispersion probability distribution takes a log-normal form:^(9, 11)

$$\mathcal{P}(t, \rho_0; d\rho) \propto e^{-\frac{1}{4D'_1 t} (\ln(\rho/\rho_0) - \lambda t)^2} d \ln \rho, \quad (2.9)$$

where $\lambda = \frac{d-4\wp}{1+2\wp} D'_1$ is the (biggest) Lyapunov exponent. It is easy to see that in this case, $\lim_{\rho_0 \rightarrow 0} \mathcal{P}(t, \rho_0; d\rho) = \delta(\rho) d\rho$, pointing to the deterministic nature of the flow. Indeed, in velocities regular in space, trajectories are uniquely determined by their initial position and very close fluid particles separate little in a fixed time interval. Nevertheless, all moments of the pair dispersion behave exponentially in time and grow in the chaotic regime where $\lambda > 0$, i.e., $\wp < d/4$, whereas sufficiently small (fractional) ones decrease when $\lambda < 0$, i.e., $\wp > d/4$. For the second moment, one obtains:

$$\langle \rho^2(t) \rangle = e^{(2\lambda + 4D'_1)t} \rho_0^2. \quad (2.10)$$

Similar behaviors persist at small times in the Kraichnan velocities with $\xi > 2$ and finite L , see ref. 28.

The stochastic Lagrangian flow occurs in the non-Lipschitz version with $0 < \xi < 2$ of the Kraichnan model for weak compressibility $\wp < d/\xi^2$. In terms of the parameter $b = \frac{1-a}{2-\xi} = \frac{2-\delta}{2}$ that will be frequently used below, the latter inequality means that $b < 1$. In this region, $\mathcal{P}(t, \rho_0; d\rho) = e^{-tM}(\rho_0, \rho) d\rho$, where M is taken with ‘‘singular Neumann’’ or reflecting boundary condition at $\rho = 0$, see ref. 23, and

$$\lim_{\rho_0 \rightarrow 0} \mathcal{P}(t, \rho_0; d\rho) \propto \rho^{a-\xi} t^{b-1} e^{-\frac{\rho^{2-\xi}}{(2-\xi)^2 D'_1 t}} d\rho. \quad (2.11)$$

Note the stretched-exponential form of the distribution. In particular, one obtains for the second moment of the separation distance and large times:

$$\langle \rho^2(t) \rangle = \mathcal{O}(t^{\frac{2}{2-\xi}}). \quad (2.12)$$

This is the Kraichnan model version of the 1926 Richardson law⁽³³⁾ stating that in developed turbulence the mean square dispersion grows like t^3 . Note that the Richardson behavior is reproduced in the Kraichnan model for $\xi = \frac{4}{3}$. In the limit when the initial trajectory separation $\rho_0 \rightarrow 0$, the power law behavior (2.12) extends to the entire time domain and $\langle \rho^2(t) \rangle \propto t^{\frac{2}{2-\xi}}$.

In the non-Lipschitz strongly compressible version of the Kraichnan model corresponding to $0 < \xi < 2$ and $\wp \geq d/\xi^2$ (or $b \geq 1$),

$$\mathcal{P}(t, \rho_0; d\rho) = \mathcal{P}^{\text{reg}}(t, \rho_0; \rho) d\rho + p(\rho_0; t) \delta(\rho) d\rho \quad (2.13)$$

with the regular density $\mathcal{P}^{\text{reg}}(t, \rho_0; \rho) = e^{-tM}(\rho_0, \rho)$ where M is taken with “singular Dirichlet” or absorbing boundary condition at $\rho = 0$, see ref. 23, and with

$$p(\rho_0; t) = 1 - \gamma\left(b, \frac{\rho_0^{2-\xi}}{(2-\xi)^2 D_1' t}\right) \Gamma(b)^{-1}, \quad (2.14)$$

where $\gamma(b, x) \equiv \int_0^x y^{b-1} e^{-y} dy$ is the incomplete gamma-function. When $\rho_0 \rightarrow 0$ then the regular part of the distribution tends to 0, whereas $p(\rho_0; t)$ tends to 1. We recover this way the deterministic behavior (2.2), with trajectories in fixed velocity realizations determined by their initial position. The presence of the singular term proportional to $\delta(\rho)$ at finite ρ_0 signals that the trajectories starting at different initial positions coalesce with positive probability.⁽²³⁾ The time growth of the mean distance square dispersion is different here:

$$\langle \rho^2(t) \rangle = \mathcal{O}(\rho_0^{1-a} t^{\frac{2}{2-\xi}-b}) \quad (2.15)$$

with a logarithmic correction at $\wp = d/\xi^2$, i.e., at $b = 1$.

2.3. Exit Time

In the Kraichnan model, the exit time distribution $\mathcal{Q}(\rho_0, \rho_1; dt)$ may also be directly controlled using the kernels $e^{-tM_D}(\rho_0, \rho)$ where M_D denotes the generator M of (2.7) with the Dirichlet boundary condition at ρ_1 (in addition to the appropriate condition at the origin when $\rho_1 > \rho_0$). This is

due to the Markov property of the stochastic process $\rho(t)$. Since the exit times have not been discussed in the context of the Kraichnan model, we shall use the occasion to provide here and in Appendix A more details, essentially translated from the Bessel diffusion case. The distribution of the time of exit through ρ_1 is given by the formula

$$\mathcal{Q}(\rho_0, \rho_1; dt) = -\partial_{n(\rho_1)} e^{-tM_D}(\rho_0, \rho) dt, \quad (2.16)$$

where $\partial_{n(\rho_1)} = \pm D_1' \rho^a \partial_\rho \rho^{\xi-a}|_{\rho=\rho_1}$ plays the same role as the normal derivative in the classical potential theory. The sign is that of $(\rho_1 - \rho_0)$. As already mentioned above, this distribution does not have to be normalized. The eventual missing mass corresponds to events where $\rho(t)$ stays forever in the intervals $[0, \rho_1)$ or (ρ_1, ∞) or when it gets absorbed at the origin, see below. We shall assign the infinite value of the exit time to such events. The averages of the powers of the exit time t over the realizations with $t < \infty$ may be expressed by the kernels of the inverse powers of operator M_D :

$$\langle t^n \mathbf{1}_{\{t < \infty\}} \rangle = \int_0^\infty t^n \mathcal{Q}(t; \rho_0, \rho_1) dt = -n! \partial_{n(\rho_1)} M_D^{-n-1}(\rho_0, \rho), \quad (2.17)$$

where by $\mathbf{1}_{\{A\}}$ we denote the characteristic functions of the events satisfying the condition A . In particular, the probability that the exit time is finite

$$\langle \mathbf{1}_{\{t < \infty\}} \rangle = \int_0^\infty \mathcal{Q}(\rho_0, \rho_1; dt) = -\partial_{n(\rho_1)} M_D^{-1}(\rho_0, \rho). \quad (2.18)$$

The expectations (2.17) may be obtained from the characteristic function

$$\langle e^{i\omega t} \mathbf{1}_{\{t < \infty\}} \rangle = -\partial_{n(\rho_1)} (M_D - i\omega)^{-1}(\rho_0, \rho) \quad (2.19)$$

involving the resolvent kernel of M_D . We shall also consider the averages conditioned on the exit times being finite:

$$\frac{\langle t^n \mathbf{1}_{\{t < \infty\}} \rangle}{\langle \mathbf{1}_{\{t < \infty\}} \rangle} \equiv \langle t^n \rangle_c, \quad \frac{\langle e^{i\omega t} \mathbf{1}_{\{t < \infty\}} \rangle}{\langle \mathbf{1}_{\{t < \infty\}} \rangle} \equiv \langle e^{i\omega t} \rangle_c. \quad (2.20)$$

For $\xi = 2$ and $L = \infty$, i.e., in the smooth version of the Kraichnan model with scaling, the kernel $e^{-tM_D}(\rho_0, \rho)$ is easily calculable by the image method and leads via Eq. (2.16) to the expression for $\mathcal{Q}(\rho_0, \rho_1; dt)$. We give the explicit formulae in Appendix A. Let us note here that $\mathcal{Q}(\rho_0, \rho_1; dt)$ has a smooth density decaying exponentially for large t and t^{-1} . It depends only on $\frac{\rho_1}{\rho_0}$ so that the Lagrangian flow is Lyapunov in our terminology, see

(2.4). The total mass of the exit time distribution is given by the simple expression:

$$\int_0^\infty \mathcal{Q}(\rho_0, \rho_1; dt) = \begin{cases} 1 & \text{if } \lambda \ln(\rho_1/\rho_0) \geq 0, \\ \left(\frac{\rho_1}{\rho_0}\right)^{\frac{\lambda}{D_1}} & \text{if } \lambda \ln(\rho_1/\rho_0) \leq 0. \end{cases} \quad (2.21)$$

The missing mass corresponds for $\rho_1 > \rho_0$ and the negative Lyapunov exponent to the events when $\rho(t)$ stays forever in the open interval $(0, \rho_1)$ (the pairs of trajectories remain always close). For $\rho_1 < \rho_0$ and the positive Lyapunov exponent, it represents the events when $\rho(t)$ stays forever in the interval (ρ_1, ∞) (the pairs of trajectories never come close). According to the characterization from the previous subsection, see conditions (2.6), the Lagrangian flow is Lyapunov, locally separating and locally transient if $\lambda > 0$, i.e., $\wp < d/4$ and it is locally trapping and locally recurrent if $\lambda < 0$, i.e., $\wp > d/4$. Finally, when $\lambda = 0$, i.e., $\wp = d/4$, it is locally separating and locally recurrent. Similar properties of the exit time distribution hold for $\xi > 2$ and finite L asymptotically at short distances.

In the non-Lipschitz version of the Kraichnan model with $0 < \xi < 2$ and $L = \infty$, the resolvent kernel $(M_D - i\omega)^{-1}(\rho_0, \rho)$ may still be easily calculated in a closed form and it leads via Eq. (2.19) to a closed expression for the Fourier transform of the exit time distribution $\mathcal{Q}(\rho_0, \rho_1; dt)$. Explicit formulae may be found in Appendix A. The density of $\mathcal{Q}(\rho_0, \rho_1; dt)$ appears to be a smooth function decaying exponentially in large t and t^{-1} if $\rho_1 > \rho_0$ and as a power of t and exponentially in t^{-1} if $\rho_1 < \rho_0$. The exit time distribution possesses the scaling property:

$$\mathcal{Q}(\mu^{2-\xi}\rho_0, \mu^{2-\xi}\rho_1; d(\mu t)) = \mathcal{Q}(t; \rho_0, \rho_1), \quad (2.22)$$

a direct consequence of the statistical scaling of the velocity differences. Relation (2.22) implies the behavior (2.5) characterizing what we have called the Richardson flows.

For $\rho_1 > \rho_0$ the total mass of the exit time distribution is

$$\langle 1_{\{t < \infty\}} \rangle = \begin{cases} 1 & \text{for } \wp < \frac{d}{\xi^2}, \\ \left(\frac{\rho_0}{\rho_1}\right)^{1-a} & \text{for } \wp \geq \frac{d}{\xi^2}. \end{cases} \quad (2.23)$$

Hence the exit time is almost surely finite in the weakly compressible regime whereas it is infinite with positive probability that depends only on

$\frac{\rho_1}{\rho_0}$ in the strongly compressible regime where the process $\rho(t)$ is absorbed at the origin with the complementary probability. Such absorption corresponds to the coalescence of pairs of trajectories. We conclude that the Lagrangian flow is locally separating for $\wp \leq d/\xi^2$ and locally trapping for $\wp > d/\xi^2$.

For $\rho_1 < \rho_0$,

$$\langle 1_{\{t < \infty\}} \rangle = \begin{cases} \left(\frac{\rho_1}{\rho_0}\right)^{a-1} & \text{for } \wp < \frac{d-2}{2\xi} + \frac{1}{2}, \\ 1 & \text{for } \wp \geq \frac{d-2}{2\xi} + \frac{1}{2}. \end{cases} \tag{2.24}$$

If $\wp < \frac{d-2}{2\xi} + \frac{1}{2}$ (i.e., if $a > 1$), the process $\rho(t)$ remains forever in the interval (ρ_1, ∞) with probability $1 - (\frac{\rho_1}{\rho_0})^{a-1} > 0$ whereas if $\wp \geq \frac{d-2}{2\xi} + \frac{1}{2}$, it exits through ρ_1 almost surely. The two situations correspond, respectively, to a locally transient and a locally recurrent Lagrangian flow.

One may summarize the properties of the Lagrangian flow in the Kraichnan model in the phase diagram, drawn in Fig. 1 for three dimensions, with five phases that we list with their characteristics (assuming for $\xi > 2$ finite L):

- I. deterministic, Lyapunov, locally separating, locally transient, for $\xi > 2$ and $\wp < d/4$;
- II. deterministic, Lyapunov, locally trapping, locally recurrent, for $\xi > 2$ and $\wp > d/4$;
- III. stochastic, Richardson, locally separating, locally transient, for $0 < \xi < 2$ and $\wp < \frac{d-2}{2\xi} + \frac{1}{2}$;

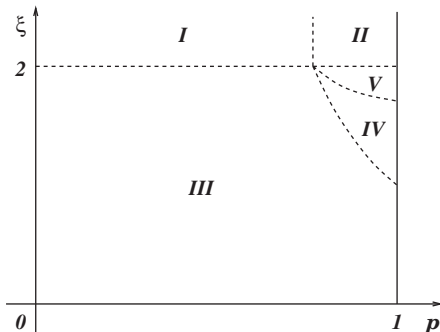


Fig. 1. Phase diagram of the Lagrangian flow for the three-dimensional Kraichnan model.

IV. stochastic, Richardson, locally separating, locally recurrent, for $0 < \xi < 2$ and $\frac{d-2}{2\xi} + \frac{1}{2} < \wp < d/\xi^2$;

V. deterministic, Richardson, locally trapping, locally recurrent, for $0 < \xi < 2$ and $d/\xi^2 < \wp$.

These phases were essentially enumerated in ref. 23 (with little stress put on the difference between phase III and IV). The characterization described above is closely related to the description of the phase diagram in ref. 28, see also ref. 12. The notable difference is that, in order to characterize the phases in the non-Lipschitz case, refs. 12 and 28 used the dichotomic behaviors of the time of exit through ρ_1 in two limits: when $\rho_1 \rightarrow 0$ with ρ_0 kept constant and when $\rho_0 \rightarrow 0$ with ρ_1 kept constant. Such behaviors enter the standard classification^(19,8) of the one-dimensional diffusion $\rho(t)$ on the half-line $[0, \infty[$ with $\rho = 0$ being, for $\xi > 2$, a natural boundary and, for $\xi < 2$, an entrance boundary in the weakly compressible phase III, a regular boundary in the intermediate phase IV and an exit boundary in the strongly compressible phase V. The use in the present paper of the small ρ_0 behavior of the exit time distribution at fixed $\frac{\rho_1}{\rho_0}$ in order to characterize the phases was motivated by the fact that such behaviors were both more amenable to analytic arguments in the presence of temporal correlations of velocities and more accessible to numerical simulations.

As noticed in ref. 12, see also ref. 29, the solution for the distribution $\mathcal{P}(t, \rho_0; d\rho)$ corresponding to the singular Dirichlet boundary condition for M and coalescent trajectories, which pertains only to phase V if the flow is defined by adding and removing small noise, sets in already in region IV if we add no noise but first smoothen out the velocity fields at short distances and subsequently remove the smoothing. Physically, the first procedure corresponds to the vanishing Prandtl and the second one to the infinite Prandtl numbers. For $\frac{d-2}{2\xi} + \frac{1}{2} < \wp < \frac{d}{\xi^2}$ and well tuned Prandtl numbers, one may also obtain intermediate solutions that correspond to a “sticky” behavior of fluid particles.⁽²⁴⁾ The different limiting procedures give then rise to different boundary conditions that may be imposed on the generator M of Eq. (2.7) in the situation when $\rho = 0$ is a regular boundary.^(8,13,19)

3. GAUSSIAN VELOCITY ENSEMBLES WITH TEMPORAL CORRELATIONS

The temporal decorrelation of the Kraichnan velocities is a simplifying feature that is quite unphysical since realistic turbulent velocities are correlated at different times. In the present paper we attempt to study the effect of temporal correlation of velocities on the behavior of the dispersion of a pair of particles in simplest ensembles of velocities with such correlations

built in. More specifically, we shall consider the Gaussian ensembles of d -dimensional velocities with mean zero and covariance

$$\langle v^i(t, \mathbf{r}) v^j(t', \mathbf{r}') \rangle = D_2 \int e^{-|t-t'| D_3 k_L^{2\beta}} \frac{e^{i\mathbf{k} \cdot (\mathbf{r}-\mathbf{r}')}}{k_L^{d+2\alpha}} P^{ij}(\mathbf{k}, \wp) \frac{d\mathbf{k}}{(2\pi)^d}. \quad (3.1)$$

There are three parameters in (3.1) not related to the choice of units: the spatial Hölder exponent α , that we shall restrict to the interval $(0, 1)$, the temporal exponent β taken positive, and the compressibility degree $\wp \in [0, 1]$. Besides, there are three dimensionful parameters: D_2 of dimension $length^{2(1-\alpha)}/time^2$, D_3 of dimension $length^{2\beta}/time$, and the integral length scale L . Similarly as in the Kraichnan ensemble, L may be taken to infinity for correlation functions of differences of velocities $\Delta v(t, \boldsymbol{\rho})$ whose statistics becomes scale invariant in this limit. The correlation time $\tau_{cr}(\rho)$ of the velocity differences in ensembles given by Eq. (3.1) is equal to $D_3^{-1} \rho^{2\beta}$ whereas the variance $\langle (\Delta v(t, \boldsymbol{\rho}))^2 \rangle \equiv \Sigma(\rho)^2$ behaves as $D_2 \rho^{2\alpha}$.

We shall be looking at the statistics of the 2-particle separation either using Eq. (1.2) with the ensemble (3.1) governing the **Eulerian** velocities, or using Eq. (1.4) with the ensemble (3.1) describing the **quasi-Lagrangian** velocities. It should be stressed that the two choices lead to two different models of Lagrangian flow. They exhibit different behaviors even for incompressible velocities where the equal-time velocity statistics of the Eulerian and quasi-Lagrangian velocities coincide. This should be contrasted with the situation in the Kraichnan model where the Eulerian and the quasi-Lagrangian velocities had the same all-time statistics so that it did not matter which one was modeled by the Gaussian ensemble (2.1). That the situation is different in the presence of temporal correlations is due to the manner in which sweeping by large scale eddies is taken into account. The 2-particle separation $\boldsymbol{\rho}$ involves only differences $\Delta v^{qL}(t, \boldsymbol{\rho})$ of the quasi-Lagrangian velocities, see (1.4). The statistics of such differences has a regular $L \rightarrow \infty$ limit if we use the Gaussian ensemble (3.1) for the quasi-Lagrangian velocities. In this case the sweeping by scale L eddies does not effect the pair dispersion. On the other hand, $\boldsymbol{\rho}$ cannot be expressed in terms of the Eulerian velocity differences only, due to the dependence on the reference trajectory $\mathbf{R}(t)$, see (1.2). As a result, if we substitute the ensemble (3.1) for the Eulerian velocities, the dispersion statistics is still effected by the scale L sweeping and behaves in a singular way in the limit $L \rightarrow \infty$. This singularity modifies also the short time behavior of the pair dispersion at fixed L in certain regimes, as we shall discuss below. The use of the synthetic ensemble (3.1) to describe turbulent velocities is in any case an approximation. It seems to render better the Lagrangian features of real turbulence if used to model the quasi-Lagrangian velocities.

In this case the large scale sweeping influences only the single particle statistics, but not the pair dispersion. We shall limit ourselves to this situation throughout most of this paper, dropping the subscript “ qL ” on the velocities. The exception is Section 7 where we discuss what happens when the Gaussian ensemble (3.1) is used to model the Eulerian velocities.

The first idea about the Lagrangian flow in the ensembles (3.1) of quasi-Lagrangian velocities may be gained by comparing the correlation time $\tau_{cr}(\rho)$ to the eddy turnover time $\tau_e(\rho) = D_2^{-1/2} \rho^{1-\alpha} \propto \rho/\Sigma(\rho)$. On the line $\alpha + 2\beta = 1$ which, in particular, contains the Kolmogorov point $\alpha = \beta = \frac{1}{3}$ (see Fig. 2), both times have the same scale dependence. For $\alpha + 2\beta < 1$ (domain C on Fig. 2), τ_{cr} becomes much shorter than τ_e at large scales and much longer at small ones. We shall see that in this domain of parameters the pair dispersion should be described at long scales (for $L = \infty$) by the Kraichnan model with rapidly decorrelating velocities and at short scales by a model with velocities independent of time (frozen). For $\alpha + 2\beta > 1$ (domains A and B on Fig. 2), the relation between the correlation times is reversed and we could expect that the frozen model controls the large scale dispersion and the decorrelated one governs the short scale behavior. A similar picture underlined the phase diagram in a simple family of scale-invariant shear flows.^(3,4) We shall study the asymptotics of the Lagrangian flow using scale transformations. Such transformations induce a flow in the plane of dimensional parameters of the model whose asymptotics is controlled by fixed points, as in the field theory renormalization group.⁽¹⁾ The perturbative renormalization group has been previously used

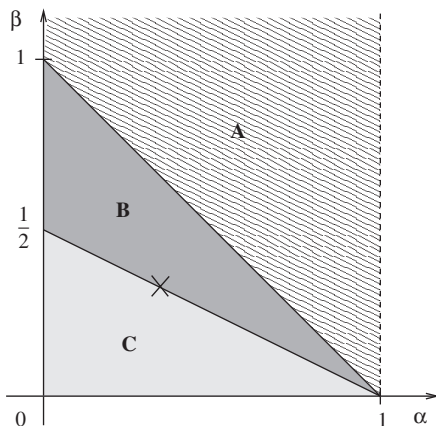


Fig. 2. Phase diagram of the three different regimes of Lagrangian flow in the time-correlated velocities discussed here. The exponent α is the spatial Hölder exponent and the exponent β controls the behavior of correlation time as a function of scale.

in ref. 2 to analyze the related scalar advection problem in the family (3.1) of velocity ensembles around $(\alpha, \beta) = (-1, 1)$ and there is some overlap of those results with our conclusions. The much heavier analysis of ref. 2 was concentrated, however, on the aspects of advection related to finer details of the Lagrangian flow, see also ref. 10. Our point is that the analysis of the Lagrangian dispersion may be performed, at least to a certain extent, in a straightforward and nonperturbative way.

The Kraichnan and the frozen model may be viewed as special limiting cases of the Gaussian velocity ensembles (3.1). The first one, with $\xi = 2(\alpha + \beta)$, is obtained when $D_2, D_3 \rightarrow \infty$ with $\frac{2D_2}{D_3} \equiv D_1$ kept constant as a consequence of the convergence

$$D_3 k_L^{2\beta} e^{-|t| D_3 k_L^{2\beta}} \xrightarrow{D_3 \rightarrow \infty} 2\delta(t). \quad (3.2)$$

At $L = \infty$, existence of the limit for the correlation functions of Δv requires that $\xi < 2$, i.e., that $\alpha + \beta < 1$. Note that the convergence is fast at large wave number k , i.e., at small distances, and for long times, but it becomes slow for short times and, if $L = \infty$, at large distances. The frozen model is obtained by taking $D_3 \rightarrow 0$ with $D_2 = \text{const}$. In this case,

$$e^{-D_3 |t| k_L^{2\beta}} \xrightarrow{D_3 \rightarrow 0} 1 \quad (3.3)$$

but the convergence becomes slow at large k , i.e., at small distances, and for long times.

Using the evolution equation (1.4) for the trajectory separation vector, we obtain for the mean rate of growth of the square of pair dispersion:

$$\frac{d}{dt} \langle \rho^2(t) \rangle = 2 \int_0^t \langle \Delta \mathbf{v}(t, \boldsymbol{\rho}(t)) \cdot \Delta \mathbf{v}(s, \boldsymbol{\rho}(s)) \rangle ds. \quad (3.4)$$

Let us start by a naive mean-field-type approximate evaluation of the right hand side in the limit when $\rho_0 \rightarrow 0$. Such an evaluation should render correctly the behavior of $\langle \rho^2(t) \rangle$ in the stochastic regime. It is obtained by rewriting Eq. (3.4) as

$$\frac{d}{dt} \langle \rho^2 \rangle = 2T \langle (\Delta \mathbf{v})^2(t, \boldsymbol{\rho}) \rangle, \quad (3.5)$$

where

$$T = \frac{\int_0^t \langle \Delta \mathbf{v}(t, \boldsymbol{\rho}(t)) \cdot \Delta \mathbf{v}(s, \boldsymbol{\rho}(s)) \rangle ds}{\langle (\Delta \mathbf{v})^2(t, \boldsymbol{\rho}(t)) \rangle}, \quad (3.6)$$

has, if smaller than t , an interpretation of the correlation time of the Lagrangian velocity difference $\Delta \mathbf{v}(t, \rho(t))$. We may try to close Eq. (3.5) by assuming that T depends on the mean separation distance $\langle \rho^2 \rangle^{1/2}$ the same way as the correlation time $\tau_{cr}(\rho)$ on ρ if $\tau_{cr}(\rho)$ is smaller than t or as t otherwise:

$$T \approx \min\{\mathcal{O}(\langle \rho^2 \rangle^\beta), t\}. \quad (3.7)$$

Different domains in the space of parameters correspond to different choices of the minimal value (3.7) for T . As for the other term on the right hand side of relation (3.5), we shall again ignore the velocity dependence of $\rho(t)$ putting

$$\langle (\Delta \mathbf{v})^2 \rangle \approx \mathcal{O}(\langle \rho^2 \rangle^\alpha). \quad (3.8)$$

Using the above approximations for **long times** and $L = \infty$, one obtains from Eq. (3.5):

$$\langle \rho^2(t) \rangle \approx \mathcal{O}(t^{\frac{2}{1-\alpha}}) \quad \text{for } \alpha + 2\beta \geq 1 \quad (\text{domains A and B}), \quad (3.9)$$

$$\langle \rho^2(t) \rangle \approx \mathcal{O}(t^{\frac{1}{1-\alpha-\beta}}) \quad \text{for } \alpha + 2\beta \leq 1 \quad (\text{domain C}). \quad (3.10)$$

In the same way, we may estimate the **short-time** behavior in the limit $\rho_0 \rightarrow 0$ obtaining

$$\langle \rho^2(t) \rangle \approx \mathcal{O}(t^{\frac{1}{1-\alpha-\beta}}) \quad \text{for } \alpha + \beta < 1 \leq \alpha + 2\beta \quad (\text{domain B}), \quad (3.11)$$

$$\langle \rho^2(t) \rangle \approx \mathcal{O}(t^{\frac{2}{1-\alpha}}) \quad \text{for } \alpha + 2\beta \leq 1 \quad (\text{domain C}). \quad (3.12)$$

Note that, in agreement with (3.7), it is the smaller exponent that is chosen for large times and the bigger one for short times, a manifestation of a tendency of close trajectories to stay close. The region $\alpha + \beta \geq 1$ (domain A in Fig. 2) which escapes the short-time estimates has been rigorously analyzed with the Gaussian ensemble (3.1) used to model the Eulerian velocities⁽¹⁸⁾ and was conjectured to correspond to deterministic trajectories. We expect that also in the quasi-Lagrangian model the pair dispersion will concentrate in domain A at $\rho = 0$ when $\rho_0 \rightarrow 0$. This is consistent with the divergence of the predicted power in the short-time Richardson law (3.12) when $\alpha + \beta$ approaches 1 from below (i.e., from the domain B in Fig. 2). A similar divergence occurs in the weakly compressible Kraichnan model when we approach the Lipschitz regime $\xi > 2$ from the non-Lipschitz one $\xi < 2$. It signals there the passage from the power law to the exponential separation (2.10) of trajectories.

4. SCALING ARGUMENTS

The main aim of this note is to substantiate further the above conclusions based on the naive estimates (3.7) and (3.8). We shall also acquire an insight into the behavior of general moments of the pair dispersion and of the exit time and into the extent of the different Lagrangian flow regimes in the ensembles given by Eq. (3.1). In the study of the long- and short-time behavior of trajectories, it is convenient to consider their rescaled versions $\mathbf{R}_\mu(t) = \mu^{-\sigma} \mathbf{R}(\mu t)$ for appropriately chosen σ . Since

$$\frac{d\mathbf{R}_\mu}{dt} = \mathbf{v}_\mu(t, \mathbf{R}_\mu), \quad (4.1)$$

for the rescaled velocity $\mathbf{v}_\mu(t, \mathbf{r}) = \mu^{1-\sigma} \mathbf{v}(\mu t, \mu^\sigma \mathbf{r})$, the path $\mathbf{R}_\mu(t)$ is a Lagrangian trajectory for \mathbf{v}_μ . There are special cases when the rescaled velocity differences have in the $L \rightarrow \infty$ limit the same distribution as the original ones for an appropriate (and unique) choice of σ . This happens for $\sigma = \frac{1}{1-\alpha}$ both on the line $\alpha + 2\beta = 1$ and in the frozen model and for $\sigma = \frac{1}{2-\xi}$ in the Kraichnan ensemble. We infer that in those cases the pair dispersion distribution \mathcal{P} and the exit time one \mathcal{Q} are scale-invariant:

$$\begin{aligned} \mathcal{P}(\mu t, \mu^\sigma \rho_0; d(\mu^\sigma \rho)) &= \mathcal{P}(t, \rho_0; d\rho), \\ \mathcal{Q}(\mu^\sigma \rho_0, \mu^\sigma \rho_1; d(\mu t)) &= \mathcal{Q}(\rho_0, \rho_1; dt). \end{aligned} \quad (4.2)$$

In particular, in the stochastic regime, the pair dispersion moments $\langle \rho(t)^n \rangle$, if finite in the $\rho_0 \rightarrow 0$ limit, behave as $\mathcal{O}(t^{n\sigma})$ for long times and become proportional to $t^{n\sigma}$ for all times when $\rho_0 \rightarrow 0$. These conclusions fail in the deterministic regime, as we have already noticed in the Kraichnan model, see Eq. (2.15). In all regimes, the exit time moments $\langle t^n 1_{\{t < \infty\}} \rangle$ (if finite) are proportional to $\rho_0^{n/\sigma}$ if $\frac{\rho_1}{\rho_0} \equiv \gamma$ is kept constant.

Out of the line $\alpha + 2\beta = 1$, the scale invariance of the Lagrangian dispersion is broken but in a predictable way, as we shall see. The crucial observation is that the rescaled velocities $\mathbf{v}_\mu(t, \mathbf{r})$ are distributed with the 2-point function (3.1) with D_i replaced by $D_{i,\mu}$ and L by L_μ , where

$$D_{2,\mu} = \mu^{2[1-(1-\alpha)\sigma]} D_2, \quad D_{3,\mu} = \mu^{1-2\beta\sigma} D_3, \quad L_\mu = \mu^{-\sigma} L. \quad (4.3)$$

For μ tending to infinity or to zero (i.e., when exploring the long-time or the short-time behavior of the particle separation), we may choose σ so that the distribution of the rescaled velocity differences at $L = \infty$ tends to the Kraichnan or to the frozen model one (with the notable exception of the $\mu \rightarrow 0$ limit in domain A).

Consider first $\mu \rightarrow \infty$ at $L = \infty$. Taking $\sigma = \frac{1}{2(1-\alpha-\beta)}$ fixes the ratio $\frac{2D_{2,\mu}}{D_{3,\mu}}$ with $D_{i,\mu} \rightarrow \infty$ if $\alpha + \beta > 1$ (domain A in Fig. 2) or if $\alpha + 2\beta < 1$ (domain C in Fig. 2). The latter case leads to a non-singular Kraichnan ensemble of velocity differences with $\xi = 2(\alpha + \beta)$ whereas the former one does not (it would correspond to $\xi > 2$, $L = \infty$). We may then expect that

$$\left. \begin{aligned} \lim_{\mu \rightarrow \infty} \mathcal{P}(\mu t, \mu^\sigma \rho_0; d(\mu^\sigma \rho)) &= \mathcal{P}^{\text{Kr}}(t, \rho_0; d\rho) \\ \lim_{\mu \rightarrow \infty} \mathcal{Q}(\mu^\sigma \rho_0, \mu^\sigma \rho_1; d(\mu t)) &= \mathcal{Q}^{\text{Kr}}(\rho_0, \rho_1; dt) \end{aligned} \right\}$$

$$\text{for } \sigma = \frac{1}{2(1-\alpha-\beta)} \text{ and } \alpha + 2\beta < 1 \quad (4.4)$$

where \mathcal{P}^{Kr} and \mathcal{Q}^{Kr} pertain to the Kraichnan model with $\xi = 2(\alpha + \beta)$. This is indeed consistent with the scaling properties of the Kraichnan model dispersion.

Taking $\sigma = \frac{1}{1-\alpha}$ fixes $D_{2,\mu}$ with $D_{3,\mu} \rightarrow 0$ if $\alpha + 2\beta > 1$ (domains A and B in Fig. 2). We then expect that

$$\left. \begin{aligned} \lim_{\mu \rightarrow \infty} \mathcal{P}(\mu t, \mu^\sigma \rho_0; d(\mu^\sigma \rho)) &= \mathcal{P}^{\text{fr}}(t, \rho_0; d\rho) \\ \lim_{\mu \rightarrow \infty} \mathcal{Q}(\mu^\sigma \rho_0, \mu^\sigma \rho_1; d(\mu t)) &= \mathcal{Q}^{\text{fr}}(\rho_0, \rho_1; dt) \end{aligned} \right\}$$

$$\text{for } \sigma = \frac{1}{1-\alpha} \text{ and } \alpha + 2\beta > 1, \quad (4.5)$$

where \mathcal{P}^{fr} and \mathcal{Q}^{fr} stand for the distributions of the frozen velocity model with Hölder exponent α . Note again the consistency with the scaling properties of the Lagrangian dispersion in the frozen model.

Inquiring about the short-time asymptotics of the trajectory dispersion reverses the asymptotics. We should then have

$$\left. \begin{aligned} \lim_{\mu \rightarrow 0} \mathcal{P}(\mu t, \mu^\sigma \rho_0; d(\mu^\sigma \rho)) &= \mathcal{P}^{\text{fr}}(t, \rho_0; d\rho) \\ \lim_{\mu \rightarrow 0} \mathcal{Q}(\mu^\sigma \rho_0, \mu^\sigma \rho_1; d(\mu t)) &= \mathcal{Q}^{\text{fr}}(\rho_0, \rho_1; dt) \end{aligned} \right\}$$

$$\text{for } \sigma = \frac{1}{1-\alpha} \text{ and } \alpha + 2\beta < 1 \quad (4.6)$$

(i.e., in domain C in Fig. 2) with the same value of the Hölder exponent α , and

$$\left. \begin{aligned} \lim_{\mu \rightarrow 0} \mathcal{P}(\mu t, \mu^\sigma \rho_0; d(\mu^\sigma \rho)) &= \mathcal{P}^{\text{Kr}}(t, \rho_0; d\rho) \\ \lim_{\mu \rightarrow 0} \mathcal{Q}(\mu^\sigma \rho_0, \mu^\sigma \rho_1; d(\mu t)) &= \mathcal{Q}^{\text{Kr}}(\rho_0, \rho_1; dt) \end{aligned} \right\}$$

$$\text{for } \sigma = \frac{1}{2(1-\alpha-\beta)} \quad \text{and} \quad \begin{cases} \alpha + \beta < 1, \\ \alpha + 2\beta > 1 \end{cases} \quad (4.7)$$

(i.e., in domain B in Fig. 2) with $\xi = 2(\alpha + \beta)$ for the Kraichnan model. Again, this is consistent with the scaling of the limiting distributions. In summary, the scale invariance of the statistics of the pair dispersion and of the exit time, although broken away from the $\alpha + 2\beta = 1$ line, should be restored at long and short times.

It has to be stressed that the relations (4.4) to (4.7) are conjectural. The distributions \mathcal{P} and \mathcal{Q} are complicated nonlinear functionals of the quasi-Lagrangian velocity statistics and the conjectured relations assume their continuity in an appropriate topology, which is not obvious. In particular, since the convergence of the rescaled velocity covariances to the one of the Kraichnan model is very slow at long distances, there is a potential threat for the corresponding convergence of the rescaled distributions $\mathcal{P}(t, \rho_0; d\rho)$ and $\mathcal{Q}(\rho_0, \rho_1; dt)$ with $\rho_1 < \rho_0$ coming from the contribution of trajectories that venture far apart, if such contributions are important. Similarly, the slow convergence to the frozen model at short distances could create problems for the corresponding convergence of the rescaled pair dispersion and exit time distributions, for the latter if $\rho_1 > \rho_0$. Whether such effects invalidate some of the conclusions (4.4) to (4.7) could be, in principle, studied in perturbation theory around the Kraichnan or frozen model. The question of the convergence of rescaled dispersion distribution to the Kraichnan model one has been recently rigorously studied in refs. 16 and 17. We shall further discuss the non-uniformity of the convergence of the exit time distributions to that of the frozen model in Section 6.

An important question concerns the **phase diagram** of the Lagrangian flow for the model (3.1) of quasi-Lagrangian velocities. As mentioned above, domain A is expected to correspond to the deterministic Lagrangian flow. The rate of separation of close trajectories in this domain (Lyapunov or Richardson flow? locally separating or trapping? locally recurrent or transient?) is also an open problem. Inside domains B and C, we may try to use the conjectured convergence (4.4) to (4.7) of the rescaled pair dispersion and time exit distributions to characterize the nature of the

Lagrangian flow. This will require even more care since some uniformity of the limits will be needed.

First, we may argue that, inside domains B and C, weak compressibility $\wp < \frac{d}{4(\alpha+\beta)^2}$ implies that the Lagrangian flow is stochastic. The argument assumes that the dichotomy “deterministic versus stochastic” may be still characterized as in Section 2, i.e., by the behavior of $\mathcal{P}(t, \rho_0; d\rho)$ in the limit $\rho_0 \rightarrow 0$. It goes as follows. Suppose that the relation (2.2) holds at some point inside B or C (for all t). Then, obviously, also

$$\lim_{\rho_0 \rightarrow 0} \mathcal{P}(\mu t, \mu^\sigma \rho_0; d(\mu^\sigma \rho)) = \delta(\rho) d\rho \quad (4.8)$$

for all μ . We expect the convergence (4.4) in domain C and (4.7) in domain B, both resulting in the Kraichnan model distributions, to be uniform at short distances and hence to commute with the $\rho_0 \rightarrow 0$ limit. We may then infer from Eq. (4.8) that (2.2) holds also for the limiting Kraichnan distribution so that $\wp \geq d/\xi^2$ where $\xi = 2(\alpha + \beta)$, which implies the assertion.

The analogous argument may be applied when

$$\lim_{\rho_0 \rightarrow 0} \int \mathcal{Q}(\rho_0, \gamma \rho_0; dt) = \lim_{\rho_0 \rightarrow 0} \int \mathcal{Q}(\mu^\sigma \rho_0, \mu^\sigma \gamma \rho_0; d(\mu t)) = 1 \quad (4.9)$$

leading to the predictions that inside the domains B and C, the Lagrangian flow is locally trapping if $\wp \geq \frac{d}{4(\alpha+\beta)^2}$ and locally transient if $\wp < \frac{d-2}{4(\alpha+\beta)} + \frac{1}{2}$. The first claim seems somewhat more trustable since it does not involve large separations where the convergence to the Kraichnan ensemble is slowed down. Both require additionally that no mass of the exit time distribution escapes to infinity during the μ -limits (4.4) and (4.7). This should not pose a problem since convergence to the Kraichnan model becomes very fast at long times.

In the stochastic regime, the convergence (4.4) and (4.7) should imply for the (positive) pair dispersion moments the behavior

$$\langle \rho^n(t) \rangle = \mathcal{O}(t^{\frac{n}{2(1-\alpha-\beta)}}) \quad (4.10)$$

for long times in domain C and for $\rho_0 \rightarrow 0$ and short times in domain B, in agreement with the naive mean-field results (3.10) and (3.11). As for the behavior of the moments of the exit time through $\gamma \rho_0$, the relations (4.7) and (4.4) should imply that

$$\langle t^n 1_{\{t < \infty\}} \rangle = \mathcal{O}(\rho_0^{2n(1-\alpha-\beta)}) \quad (4.11)$$

in domain B for small ρ_0 and in domain C for large ones, irrespectively of the character of the Lagrangian flow. Similarly, we should obtain in domain B the convergence

$$\lim_{\mu \rightarrow 0} \int f(t) \mathcal{Q}(\mu^\sigma \rho_0, \mu^\sigma \gamma \rho_0; dt) = f(0) \int \mathcal{Q}^{\text{Kr}}(\rho_0, \rho_1; dt) \quad (4.12)$$

characteristic of the Richardson flow in our terminology.

Similar use of the conjectured convergences (4.5) and (4.6) to the frozen model distributions in order to argue about the Lagrangian flow dichotomies and the evolution of dispersion and exit times moments poses two problems. First is the poor knowledge of the flow behavior in the frozen model, see, however, Section 5. Second, even more serious one, is the non-uniform nature of the convergence that becomes slow at small distances and long times. Nevertheless, it is still plausible that the convergence (4.5) is uniform enough as to imply that

$$\langle \rho^n(t) \rangle = \mathcal{O}(t^{\frac{n}{1-\alpha}}) \quad (4.13)$$

for long times and for sufficiently high n in the stochastic regime in domains A and B. Similarly, relations (4.5) and (4.6) may still imply that for sufficiently negative moments,

$$\langle t^n \rangle = \mathcal{O}(\rho_0^{n(1-\alpha)}) \quad (4.14)$$

in domains A and B for large ρ_0 and in domain C for small ones, see Section 6. The same way, the convergence (4.12) should still hold in domain C for test functions f decaying fast at infinity and \mathcal{Q}^{Kr} replaced by \mathcal{Q}^{fr} .

Summarizing, we predict, with various level of confidence, that the (zero Prandtl number) Lagrangian flow in the quasi-Lagrangian velocity ensemble (3.1) is

deterministic
in domain A

stochastic, Richardson, locally transient
in domains B and C for $\wp < \frac{d-2}{4(\alpha+\beta)} + \frac{1}{2}$,

stochastic, Richardson
in domains B and C for $\frac{d-2}{4(\alpha+\beta)} + \frac{1}{2} \leq \wp < \frac{d}{4(\alpha+\beta)^2}$,

Richardson, locally trapping
in domains B and C for $\wp \geq \frac{d}{4(\alpha+\beta)^2}$.

The degree of confidence of the predictions depends on which of relations (4.4) to (4.7) was used in the argument and with what uniformity assumptions. The predictions are consistent with the intuition that increase of the compressibility degree \wp enhances the trapping of the fluid particles. It will be interesting to confirm (or infirm) them by further analytic arguments and by numerical simulations. Note that, in particular, we expect that in domains B and C the incompressible Lagrangian flow is stochastic, Richardson and locally transient, and that, if the dimension $d \geq 4$, it stays such, whatever compressibility.

5. ONE-DIMENSIONAL FROZEN ENSEMBLE

The frozen model was left out from the discussion of the phase diagram in the last section. Our arguments were based mainly on the convergence of the rescaled velocity ensemble (3.1) to the Kraichnan model and such convergence is, of course, absent for the frozen model. One may expect appearance of discontinuity in the character of the Lagrangian flow in the frozen model limit $D_3 \rightarrow 0$ which is very non-uniform at short distances and long times, leading to a strong enhancement of trapping. This effect will be analyzed in the next section. Here we shall try to find out what happens in the frozen velocities which, in general, are hard to analyze. One case where some analytic results may be obtained due to the very simple geometry of the flow is the one-dimensional Gaussian model where the Lagrangian particles slide down the potential wells, getting stuck at their bottom, and where the flow preserves the order of particles. In particular, when the spatial Hölder exponent $\alpha = \frac{1}{2}$, the velocity 2-point function becomes

$$\langle v(x) v(y) \rangle = \int \frac{e^{ik(x-y)}}{k^2 + L^{-2}} \frac{dk}{2\pi} = \frac{1}{2} L e^{-|x-y|/L}, \quad (5.1)$$

where we have set $D_2 = 1$ (what may be always achieved by rescaling $v \mapsto \sqrt{D_2} v$). The additional simplifying feature of this case, studied already in ref. 34, is that $v(x)$ forms a stationary Markov (Ornstein–Uhlenbeck) process with the generator

$$\mathcal{L} = -\frac{1}{2} \frac{d^2}{dv^2} + \frac{v}{L} \frac{d}{dv} \quad (5.2)$$

corresponding to the Focker–Planck harmonic oscillator Hamiltonian

$$\mathcal{H} = e^{-\frac{v^2}{2L}} \mathcal{L} e^{\frac{v^2}{2L}} = -\frac{1}{2} \frac{d^2}{dv^2} + \frac{v^2}{2L^2} - \frac{1}{2L}. \quad (5.3)$$

The velocity $v(x)$ with fixed x is distributed according to the invariant measure of the process

$$dv(v) = \frac{1}{\sqrt{\pi L}} e^{-\frac{v^2}{L}} dv. \quad (5.4)$$

The transition probabilities of the process are

$$p(t, v_0; dv) = e^{-t\mathcal{L}}(v_0, v) dv = \frac{1}{\sqrt{\pi L(1 - e^{-2t/L})}} e^{-\frac{(e^{-t/L}v_0 - v)^2}{L(1 - e^{-2t/L})}} dv. \quad (5.5)$$

In the limit $L \rightarrow \infty$, the velocity difference $\Delta v(x) = v(x) - v(0)$ becomes the one-dimensional two-sided Brownian motion $w(x)$. The quasi-Lagrangian Eq. (1.4) for the trajectory separation takes then the form of the steepest descent equation

$$\frac{d\rho}{dt} = w(\rho) = -\frac{d}{d\rho} \phi(\rho). \quad (5.6)$$

in the potential $\phi(x) = -\int_0^x w(y) dy$. The solution $\rho(t)$ slides to the bottom of the potential well in which the initial point $\rho_0 = \rho(0)$ is situated, i.e., to the closest zero ρ_+ of $w(\rho)$ to the right of ρ_0 if $w(\rho_0) > 0$ or ρ_- to the left of ρ_0 if $w(\rho_0) < 0$. The only difference with the case of smooth potential with wells approximately quadratic around typical minima, is that, as we show below, the solution will arrive to the bottom of the well in a finite rather than infinite time. This is due to the roughness of the Brownian motion. After arriving at the bottom, the solution will stay locked there in subsequent times.

We may restrict ourselves to the case $\rho_0 > 0$. Suppose also that $w(\rho_0) > 0$. The first value ρ_+ to the right of ρ_0 such that $w(\rho_+) = 0$ is finite with probability one. The time t_+ that the solution $\rho(t)$ of Eq. (5.6) starting at ρ_0 at time zero takes to reach ρ_+ is

$$t_+ = \int_{\rho_0}^{\rho_+} \frac{d\rho}{w(\rho)}. \quad (5.7)$$

Let us compute the expectation $\langle t_+ 1_{\{w(\rho_0) > 0, \rho_+ \leq \rho_2\}} \rangle$ of times t_+ over the Brownian paths $w(\rho)$ such that $w(\rho_0) > 0$ and $\rho_+ \leq \rho_2$ for certain $\rho_2 > \rho_0$. It is equal to

$$\int_{\rho_0}^{\rho_2} d\rho \int_0^\infty e^{-\frac{w_0^2}{2\rho_0}} \frac{dw_0}{\sqrt{2\pi\rho_0}} \int_0^\infty \left(e^{-\frac{(w_0-w)^2}{2(\rho-\rho_0)}} - e^{-\frac{(w_0+w)^2}{2(\rho-\rho_0)}} \right) \frac{dw}{\sqrt{2\pi(\rho-\rho_0)} w} \times \int_0^\infty e^{-\frac{(w+w_2)^2}{2(\rho_2-\rho)}} \frac{2 dw_2}{\sqrt{2\pi(\rho_2-\rho)}}. \tag{5.8}$$

The origin of this formula is straightforward. The probability that $w(\rho_0)$ belongs to $[w_0, w_0 + dw_0]$ is $e^{-\frac{w_0^2}{2\rho_0}} \frac{dw_0}{\sqrt{2\pi\rho_0}}$. The one that $w(\rho)$ belongs to $[w, w + dw]$ without passing through zero between ρ_0 and ρ is $(e^{-\frac{(w_0-w)^2}{2(\rho-\rho_0)}} - e^{-\frac{(w_0+w)^2}{2(\rho-\rho_0)}}) \frac{dw}{\sqrt{2\pi(\rho-\rho_0)}}$, given that $w(\rho_0) = w_0$, (it is expressed by the heat kernel with the Dirichlet condition at $w = 0$). Finally, the last integral on the right hand side of (5.8) is equal to the probability that the Brownian trajectory crosses zero between ρ and ρ_2 , given that $w(\rho) = w$. In Appendix B we show that

$$\langle t_+ 1_{\{w(\rho_0) > 0, \rho_+ \leq \rho_2\}} \rangle \leq C_+ \rho_0^{1/2} \ln \frac{\rho_2}{\rho_0}, \tag{5.9}$$

where C_+ is a dimensionless constant. This proves that the time t_+ is almost surely finite although the unrestricted mean $\langle t_+ 1_{\{w(\rho_0) > 0\}} \rangle$, given by the $\rho_2 \rightarrow \infty$ limit of (5.8) under which the last integral on the right hand side tends to one, diverges. The divergence is due to the contribution of the Brownian paths that travel far before falling back to zero. In the Ornstein–Uhlenbeck process with $L < \infty$, the weight of such paths is suppressed and it is not difficult to show that $\langle t_+ 1_{\{w(\rho_0) > 0\}} \rangle$ is finite then.

Similarly, let $w(\rho_0) < 0$ and $0 \leq \rho_- < \rho_0$ be the first value to the left of ρ_0 such that $w(\rho_-) = 0$. The time t_- that the solution $\rho(t)$ of Eq. (5.6) starting at ρ_0 at time zero takes to reach ρ_- is given by Eq. (5.7) with t_+ replaced by t_- and ρ_+ by ρ_- . The expectation value $\langle t_- 1_{\{w(\rho_0) < 0\}} \rangle$ is given by

$$-\int_0^{\rho_0} d\rho \int_{-\infty}^0 e^{-\frac{w^2}{2\rho}} \frac{dw}{\sqrt{2\pi\rho} w} \int_{-\infty}^0 \left(e^{-\frac{(w-w_0)^2}{2(\rho_0-\rho)}} - e^{-\frac{(w+w_0)^2}{2(\rho_0-\rho)}} \right) \frac{dw_0}{\sqrt{2\pi(\rho_0-\rho)}} \tag{5.10}$$

which is easily seen to be finite, e.g., by bounding the last integral by $\sqrt{\frac{2}{\pi(\rho_0 - \rho)}} |w|$. We infer that

$$\langle t_- 1_{\{w(\rho_0) < 0\}} \rangle = C_- \rho_0^{1/2}, \quad (5.11)$$

where C_- is another dimensionless constant.

5.1. Exit Time

As for the exit time that the process $\rho(t)$ takes to grow from ρ_0 to $\rho_1 > \rho_0$, it is finite if and only if $\rho(t)$ is not stuck at a zero $\rho_{\pm} < \rho_1$ of $w(\rho)$, i.e., if w is positive on the interval $[\rho_0, \rho_1)$. It is then given by the formula

$$t = \int_{\rho_0}^{\rho_1} \frac{d\rho}{w(\rho)}. \quad (5.12)$$

The probability that $t < \infty$ is given by

$$\langle 1_{\{t < \infty\}} \rangle = \int_0^{\infty} e^{-\frac{w_0^2}{2\rho_0}} \frac{dw_0}{\sqrt{2\pi\rho_0}} \int_0^{\infty} \left(e^{-\frac{(w_0 - w_1)^2}{2(\rho_1 - \rho_0)}} - e^{-\frac{(w_0 + w_1)^2}{2(\rho_1 - \rho_0)}} \right) \frac{dw_1}{\sqrt{2\pi(\rho_1 - \rho_0)}}. \quad (5.13)$$

Note that the last expression depends only on $\frac{\rho_1}{\rho_0}$, is smaller than 1/2 and tends to zero when $\rho_0 \rightarrow 0$ with ρ_1 fixed. With the complementary probability, the solution $\rho(t)$ starting from $\rho_0 > 0$ will never reach ρ_1 , i.e., the exit time t is infinite. One may express similarly the averages of positive powers of the exit time constraint to be finite. The explicit expression may be found in Appendix C. They are finite and take the scaling form

$$\langle t^n 1_{\{t < \infty\}} \rangle = C_n \tau_e^n \quad (5.14)$$

where C_n are dimensionless constants depending on the ratio $\gamma = \frac{\rho_1}{\rho_0} > 1$ and $\tau_e = (\rho_0/D_2)^{1/2}$ is the eddy turnover time at scale ρ_0 (recall that we have set $D_2 = 1$ above).

The bounds (C.2) for the moments $\langle t^n 1_{\{t < \infty\}} \rangle$ proven in Appendix C, which respect the above scaling, imply that the characteristic function $\langle e^{i\omega t} 1_{\{t < \infty\}} \rangle$ is entire in ω and that the large t decay of the density of the distribution $\mathcal{Q}(\rho_0, \rho_1; dt)$ is at least Gaussian. Due to Eq. (5.12), the characteristic function may be expressed by the path integral

$$\langle e^{i\omega t} 1_{\{t < \infty\}} \rangle = \frac{1}{\mathcal{N}} \int_0^{\infty} e^{-\frac{w_0^2}{2\rho_0}} \frac{dw_0}{\sqrt{2\pi\rho_0}} \int e^{\int_{\rho_0}^{\rho_1} \left(\frac{i\omega}{w(\rho)} - \frac{1}{2} w^2(\rho) \right) d\rho} \mathcal{D}w \quad (5.15)$$

over the paths $[\rho_0, \rho_1] \ni \rho \mapsto w(\rho) \in (0, \infty)$ such that $w(\rho_0) = w_0$, with \mathcal{N} being an appropriate normalization factor. The expression permits to evaluate the large $|\omega|$ -behavior along the positive imaginary axis of ω by the semi-classical calculation. The extremal trajectory $w(\rho)$ describes a motion of a unit mass particle climbing up in the potential $-\frac{1}{w}$ until a total stop. It satisfies the equation

$$\frac{\sin \varphi_0}{\cos^3 \varphi_0} (\varphi + \sin \varphi \cos \varphi) = \frac{\rho_1}{\rho_0} - \frac{\rho}{\rho_0} \quad (5.16)$$

for $\cos^2 \varphi = \frac{w(\rho)}{w(\rho_1)}$, $\cos^2 \varphi_0 = \frac{w(\rho_0)}{w(\rho_1)}$ and φ between zero and $\varphi_0 < \frac{\pi}{2}$. In particular, φ_0 is determined by Eq. (5.16) with $\varphi = \varphi_0$ and $\rho = \rho_0$. It depends only on the ratio $\frac{\rho_1}{\rho_0}$. The action of the classical trajectory is $S_0 = |\omega|^{2/3} \rho_0^{1/3} s_0$ with a dimensionless constant $s_0 = \frac{3\varphi_0 \sin^{1/3} \varphi_0}{2^{1/3} \cos \varphi_0}$ growing with the $\frac{\rho_1}{\rho_0}$. The decay $\sim e^{-S_0}$ of the characteristic function along the positive imaginary axis corresponds to the small t behavior $\sim e^{-\frac{4}{27} \rho_0^3 t^{-2}} = e^{-\frac{4}{27} s_0^3 (\tau_e/t)^2}$ of the density of the exit time distribution $\mathcal{Q}(\rho_0, \rho_1; dt)$ (up to powers of t). One could expect that for short times the trajectories move almost ballistically:

$$\rho(t) \simeq \rho_0 + w(\rho_0) t \quad (5.17)$$

which would give $t \simeq \frac{\rho_1 - \rho_0}{w(\rho_0)}$ and a short time tale $\sim e^{-\frac{(\rho_1 - \rho_0)^2}{2\rho_0} t^{-2}}$ of the exit time density function. This reproduces well the power of t in the exponential but not the coefficient. The latter, divided by ρ_0 , agrees only to the order $(\frac{\rho_1}{\rho_0} - 1)^2$ with the correct expression $\frac{4}{27} s_0^3$.

For ω on the imaginary axis, the path-integral on the right hand side of Eq. (5.15) may be re-expressed in the operator language via the Feynman–Kac formula. Using also the invariance of the Brownian motion under the scale transformations $w(x) \mapsto |\omega|^{-1} w(|\omega|^2 x)$, we obtain the identity

$$\langle e^{i\omega t} 1_{\{t < \infty\}} \rangle = \int_0^\infty e^{-\frac{w_0^2}{2|\omega|^2 \rho_0}} \frac{dw_0}{\sqrt{2\pi\rho_0} |\omega|} \int_0^\infty e^{-|\omega|^2 (\rho_1 - \rho_0) \mathcal{K}_\pm(w_0, w_1)} dw_1, \quad (5.18)$$

where the operator

$$\mathcal{K}_\pm = -\frac{1}{2} \frac{d^2}{dw^2} \pm \frac{1}{w} \quad (5.19)$$

on the interval $[0, \infty)$ is a 1-dimensional Schrödinger operator with Dirichlet boundary condition at zero. The signs pertain to the positive or

negative imaginary ω -axis and result in a repulsive or an attractive potential, respectively. An explicit expression for the kernel of the exponential of \mathcal{K}_- , see Appendix D, shows the growth of the characteristic function for $\omega = -i |\omega|$ dominated by the lowest bound state contribution $\sim e^{-|\omega|^2 (\rho_1 - \rho_0) E_0}$ with $E_0 = -\frac{1}{2}$. This implies the decay $\sim e^{-\frac{1}{(\rho_1 - \rho_0)} t^2} = e^{-\frac{1}{\gamma-1} (t/\tau_e(\rho_0))^2}$ of the density of $\mathcal{Q}(\rho_0, \rho_1; dt)$ for large t .

The above analytic predictions may be used to validate the numerical method to be applied later for the cases $\alpha \neq 1/2$, where such rigorous results are not available. The velocity field is generated by using a straightforward Fourier method, i.e., generating the Fourier modes by a standard Gaussian random number generator and transforming back to real space by Fast Fourier Transform. The resolution which we used was 2^{20} . The initial separation is set at 20,000 and we measure the distribution of the time taken to reach 5 times the initial separation. The curve is shown in Fig. 3. The agreement with the superposed predictions indicates that the choice of the resolution and the initial separation are appropriate to avoid contamination by periodicity and/or discretization effects.

The time in which $\rho(t)$ decreases from ρ_0 to a positive value $\rho_1 < \rho_0$ is finite and still determined by Eq. (5.12) if and only if $w < 0$ on the interval $(\rho_1, \rho_0]$. It is easy to see that

$$\mathcal{Q}(\rho_0, \rho_1; dt) = \mathcal{Q}(\rho_1, \rho_0; dt) \tag{5.20}$$

since for $\rho_1 < \rho_0$ the characteristic function $\langle e^{i\omega t} 1_{\{t < \infty\}} \rangle$ is given by the expression (5.15) with ρ_0 and ρ_1 interchanged.

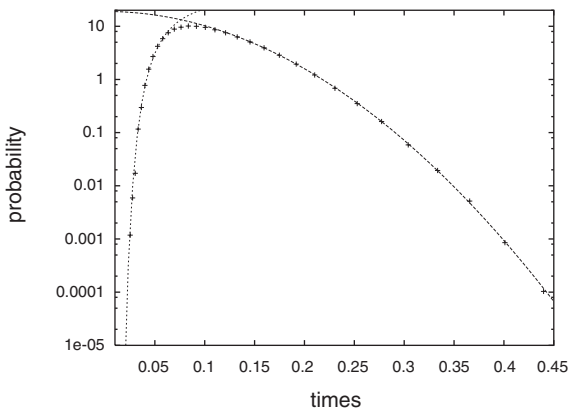


Fig. 3. The density function of the exit times for the frozen flow with $\alpha = \frac{1}{2}$ and $\gamma = 5$. The dotted curves are the analytical predictions at small and large times, respectively.

The scaling property (4.2) with $\sigma = 2$ and the fact that the exit time is infinite with a positive probability depending on $\frac{\rho_1}{\rho_0}$ imply that

$$\lim_{\rho_0 \rightarrow 0} \mathcal{Q}(\rho_0, \gamma \rho_0; dt) = c(\gamma) \delta(t) dt \quad (5.21)$$

for any positive $\gamma \neq 1$ with $0 < c(\gamma) < 1$. It follows that the Lagrangian flow is Richardson, locally trapping and locally transient in the terminology of Section 2.1.

5.2. Pair Dispersion

The pair dispersion in the model is closely related to the exit time. The reason is that the solution $\rho(t)$ of Eq. (5.6) never changes direction. As a result, the solution that starts at ρ_0 at time zero satisfies $\rho(t) \geq \rho_1 \geq \rho_0$ or $\rho(t) \leq \rho_1 \leq \rho_0$ if and only if it reaches ρ_1 in time shorter or equal to t . It follows that

$$\int_{\rho_1}^{\infty} \mathcal{P}(t, \rho_0; d\rho) = \int_0^t \mathcal{Q}(\rho_0, \rho_1; ds) \quad \text{for } \rho_1 \geq \rho_0, \quad (5.22)$$

$$\int_0^{\rho_1} \mathcal{P}(t, \rho_0; d\rho) = \int_0^t \mathcal{Q}(\rho_0, \rho_1; ds) \quad \text{for } \rho_1 \leq \rho_0 \quad (5.23)$$

or that

$$\mathcal{P}(t, \rho_0; d\rho) = \mp \left(\partial_\rho \int_0^t \mathcal{Q}(\rho_0, \rho; ds) \right) d\rho \quad \text{for } \rho \geq \rho_0. \quad (5.24)$$

The right hand side of Eq. (5.22) is bounded by $\int_0^\infty \mathcal{Q}(\rho_0, \rho_1; ds)$ which tends to zero when $\rho_0 \rightarrow 0$ for $\rho_1 > 0$ fixed, see Eq. (5.13). It follows that

$$\lim_{\rho_0 \rightarrow 0} \mathcal{P}(t, \rho_0; d\rho) = \delta(\rho) d\rho, \quad (5.25)$$

in agreement with the fact that the trajectories are determined by the initial condition. Hence the Lagrangian flow is deterministic. Note the important difference with the phase V of the Kraichnan model, see Fig. 1. There the trapping effects resulted in the coalescence of fluid particles signaled by the singular form (2.13) of the pair dispersion distribution. With the use of symmetry (5.20), the left hand side of Eq. (5.23) may be bounded by $\int_0^\infty \mathcal{Q}(\rho_1, \rho_0; ds)$ and hence tends to zero when $\rho_1 \rightarrow 0$ for fixed $\rho_0 > 0$. As a result, the distribution $\mathcal{P}(t, \rho_0; d\rho)$ cannot have a contribution proportional to $\delta(\rho)$ for $\rho_0 > 0$. It is, instead, regular in ρ . The reason is that in the

quasi-Lagrangian model of particle separation (5.6), the solutions $\rho(t)$ are trapped with probability 1 at positive zeros of w (there is an infinity of such zeros) and never arrive at $\rho = 0$. This seems to be an artifact of the frozen one-dimensional model but it serves as a warning that the behavior of trajectories in the time-correlated velocities may be richer than what was observed for the Kraichnan model, with a possible occurrence of phase

VI. deterministic, Richardson, locally trapping, locally transient

characterized by a combination of properties that did not occur in the time-decorrelated model.

5.3. Case with $\alpha \neq \frac{1}{2}$

Several of the features analytically established for the one-dimensional frozen model with the Hölder exponent $\alpha = \frac{1}{2}$ may be generalized to the case of general α in the interval $(0, 1)$, although the absence of the Markov property in the process $v(x)$ makes the arguments more difficult, see ref. 25. In the limit $L \rightarrow \infty$, the equation for the trajectory separation still has the form (5.6) with $w(x)$, $x \geq 0$, being (upon a right choice of the normalization constant D_2) the two-sided **fractional Brownian motion** (fBm), i.e., the Gaussian process with mean zero and 2-point function

$$\langle w(x) w(y) \rangle = \frac{1}{2} (x^{2\alpha} + y^{2\alpha} - |x - y|^{2\alpha}) \equiv G(x, y) \quad (5.26)$$

for $x, y \geq 0$. The 2-point function (5.26) is a kernel of a positive operator on the half-axis $[0, \infty)$ that we shall denote by G . Note the scale invariance under $w(x) \mapsto \mu^{-\alpha} w(\mu x)$ of the fBm. The basic result of ref. 31 asserts that the probability that $w(x) < w_0$ for $w_0 > 0$ and all x in the interval $(0, \rho_0)$ behaves like $\mathcal{O}((\rho_0 w_0^{-1/\alpha})^{1-\alpha})$ for large values of $\rho_0 w_0^{-1/\alpha}$. Similarly as for the Brownian motion, the fBm lives on continuous trajectories and has zeros in any interval $(0, \rho_0)$ or (ρ_0, ∞) . One may again prove that, with probability 1, the solution $\rho(t)$ of Eq. (5.6) starting at any $\rho_0 > 0$ arrives in finite time at the closest zero ρ_{\pm} to the right or left of ρ_0 , see ref. 25.

As in the case $\alpha = \frac{1}{2}$, the exit time t through $\rho_1 > \rho_0$ is finite if and only if $w > 0$ on the interval $[\rho_0, \rho_1)$ and the probability $\langle 1_{\{t < \infty\}} \rangle$ of such an event depends only on $\frac{\rho_1}{\rho_0}$ and tends to zero when $\rho_0 \rightarrow 0$. It should be again possible to extract the behaviors of the exit time distribution $\mathcal{Q}(\rho_0, \rho_1; dt)$ for large and small time by looking at the large $|\omega|$ behavior of

$$\langle e^{\pm|\omega|t} 1_{\{t < \infty\}} \rangle = \langle e^{\pm|\omega| \int_{\rho_0}^{\rho_1} \frac{dp}{w(p)}} 1_{\{w > 0 \text{ on } [\rho_0, \rho_1)\}} \rangle, \quad (5.27)$$

where the last expectation is with respect to the Gaussian measure of the fBm w . For the negative sign, this expression should be still dominated for large $|\omega|$ by the semi-classical contribution $\sim e^{-S_0}$. The classical trajectory $w(\rho) = |\omega|^{1/3} \rho_0^{(1+2\alpha)/3} (Gu)(\frac{\rho}{\rho_0})$, where u is a function that does not vanish only on the interval $(1, \frac{\rho_1}{\rho_0})$ and such that

$$u = (Gu)^{-2} \quad (5.28)$$

there. Note that it follows that $w(\rho) > 0$ for $\rho > 0$ since $G(x, y) > 0$ except for $x, y = 0$. The action of the classical trajectory is $S_0 = |\omega|^{2/3} \rho_0^{2(1-\alpha)/3} s_0$ for

$$s_0 = \int_1^{\rho_1/\rho_0} \left[\frac{1}{(Gu)(x)} + \frac{1}{2} u(x) (Gu)(x) \right] dx. \quad (5.29)$$

Such a semi-classical dominance implies again the small time tail $\sim e^{-\frac{4}{27} \rho_0^{2(1-\alpha)} s_0^3 t^{-2}} = e^{-\mathcal{O}((\tau_e/t)^2)}$ of the density of the exit time distribution $\mathcal{Q}(\rho_0, \rho_1; dt)$ (with the eddy turnover time $\tau_e = D_2^{-1/2} \rho_0^{1-\alpha}$).

With the use of the scale invariance of the fBm, one may also absorb the $|\omega|$ -dependence of the characteristic function into the length of the ρ -interval in Eq. (5.27):

$$\langle e^{\pm|\omega|t} 1_{\{t < \infty\}} \rangle = \langle e^{\pm \int_{\rho_0}^{\rho_1} \frac{d\rho}{w(\rho)}} 1_{\{w > 0 \text{ on } [\rho_0', \rho_1']\}} \rangle, \quad (5.30)$$

where $\rho_i' = |\omega|^{1/(1-\alpha)} \rho_i$. For the positive sign in Eq. (5.30) and $\alpha = \frac{1}{2}$, we have used the Feynman–Kac formula in order to extract the extensive behavior of the right hand side for large $|\omega|$. For other values of $\alpha \in (0, 1)$ such a formula is not available but the expectation (5.30) may be viewed as the partition function of a one-dimensional continuous spin system with long-range 2-spin interactions decaying as *distance*^{-2(1+ α)} and with partially confining (as opposed to the case with negative sign) single-spin potential. It is plausible that the extensive behavior of the partition function $\sim e^{-|\omega|^{1/(1-\alpha)} (\rho_1 - \rho_0) E_0}$ for large $|\omega|$ with free energy density $E_0 < 0$ persists for such systems. Such a behavior would result in the long-time tail $\sim e^{-\alpha \left(\frac{1-\alpha}{|\rho_1 - \rho_0| E_0} \right)^{(1-\alpha)/\alpha} t^{1/\alpha}} = e^{-\mathcal{O}((t/\tau_e)^{1/\alpha})}$ of the density of the distribution $\mathcal{Q}(\rho_0, \rho_1; dt)$. The validity of this prediction is confirmed by Figs. 4 and 5 where we present the density functions of the exit times for the two cases $\alpha = 0.4$ and 0.75 . The numerical simulations are realized by the same method previously validated in the case $\alpha = \frac{1}{2}$. It requires for $\alpha \neq \frac{1}{2}$ more care in the choice of parameters to maximize the scaling window.

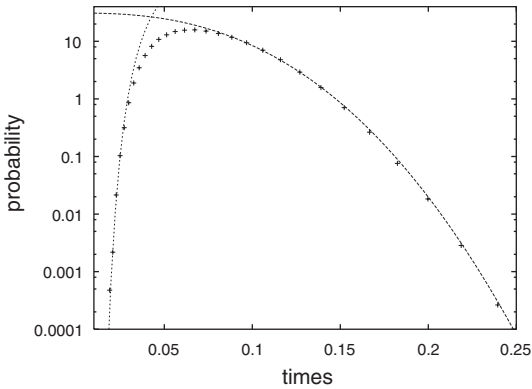


Fig. 4. The density function of the exit times for the $1d$ frozen velocities with $\alpha = 0.4$ and $\gamma = 5$. The dotted curve is a fit of the form $e^{-\text{const. } t^{1/\alpha}}$.

The statistics of the time of exit through $\rho_1 < \rho_0$ is again obtained from that for $\rho_1 > \rho_0$ by interchanging ρ_0 and ρ_1 and the pair dispersion probability distribution is still given by Eq. (5.24). The remarks about the phase VI type behavior of Lagrangian flow carry over from the case $\alpha = \frac{1}{2}$.

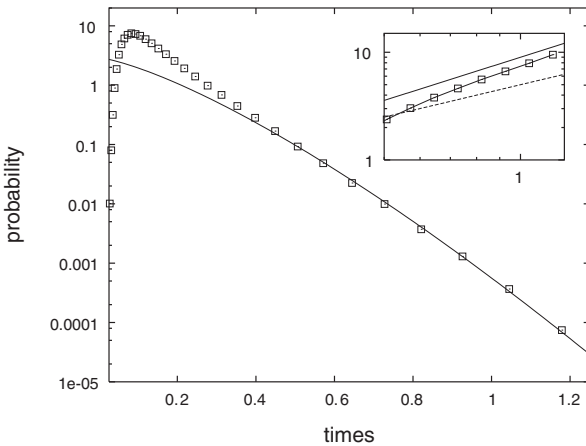


Fig. 5. The density function of the exit times for the $1d$ frozen velocities with $\alpha = 3/4$ and $\gamma = 5$. The solid curve is a fit of the form $e^{-\text{const. } t^{1/\alpha}}$. Since the curve gives the visual impression of an exponential decay, we also show in the inset the log log vs log plot and compare the slopes 0.75 and 1 to validate the former.

6. EFFECT OF LONG TIME VELOCITY CORRELATIONS

The presence of permanent trapping of trajectories in one-dimensional frozen ensemble, leading to events with infinite exit time through $\rho_1 = \gamma\rho_0$, should also occur in higher-dimensional frozen ensembles obtained by setting $D_3 = 0$ in Eq. (3.1). It is plausible that, at least in the presence of compressibility, the sets of velocities trapping trajectories in a given region have positive probability. If, however, one reintroduces finite temporal correlations of velocities by taking positive D_3 in (3.1), the particles will eventually be released from traps after the time evolution changes the velocity field configuration, i.e., after time of order $\tau_{cr}(\rho) = D_3^{-1}\rho^{2\beta}$ for traps of size ρ . If for $D_3 > 0$ the exit times are finite so that $\int_0^\infty \mathcal{Q}(dt) = 1$, then the missing mass $1 - \int_0^\infty \mathcal{Q}(dt) > 0$ for $D_3 = 0$ should be built from the long-time tails of the density of \mathcal{Q} at positive D_3 , as the latter is taken to zero. Loosely speaking, we may then expect that for fixed ρ_0, γ , and D_2 ,

$$\mathcal{Q}(\rho_0, \gamma\rho_0; dt) \approx \mathcal{Q}^\infty(\gamma; d(t/\tau_{cr})) \quad \text{for } t/\tau_{cr} \gg 1. \quad (6.1)$$

with $\tau_{cr} = \tau_{cr}(\rho_0)$ and the density of \mathcal{Q}^∞ having a (Poissonian) exponential tail. Let us concentrate on the one-dimensional situation where the frozen exit-time density function is expected to have a stretched exponential tail $\sim e^{-\mathcal{O}((t/\tau_e)^{1/\alpha})}$ with the scale set by the eddy turnover time $\tau_e = D_2^{-1/2}\rho_0^{1-\alpha}$. Note that the latter attains the value of order τ_{cr}^{-1} for $t = \tau'$ with $\tau'/\tau_e = \mathcal{O}((\ln(\tau_{cr}/\tau_e))^\alpha) = \mathcal{O}(|\ln D_3|^\alpha)$. The ‘‘minimal’’ scenario would be that the frozen density function passes into the form of (6.1) around $t = \tau'$. More precisely, we may postulate the convergence

$$\begin{aligned} \mathcal{Q}(\rho_0, \gamma\rho_0; dt) 1_{\{t < \tau'\}} \xrightarrow{D_3 \rightarrow 0} \mathcal{Q}^{\text{fr}}(\rho_0, \gamma\rho_0; dt) \\ \mathcal{Q}(\rho_0, \gamma\rho_0; d(s\tau_{cr})) 1_{\{s \geq \tau'/\tau_{cr}\}} \xrightarrow{D_3 \rightarrow 0} \mathcal{Q}^\infty(\gamma; ds) \end{aligned} \quad (6.2)$$

in a strong enough sense. The above relations imply that the large exit time behavior becomes self-similar for small D_3 , with the characteristic scale equal to τ_{cr} , with no intermediate regime between the frozen type behavior and the self-similar tail. It is also possible that a different intermediate regime sets in between times of order τ' and τ_{cr} , with τ' depending differently on D_3 .

The minimal scenario would make explicit the large t non-uniformity of the conjectured convergence of the exit time distributions, see (4.5) and (4.6). Recall that the conjecture was based on the scaling relation that may be rewritten as the identity

$$\mathcal{Q}(\rho_0, \gamma\rho_0; d(\rho_0^{1-\alpha}t))|_{D_3} = \mathcal{Q}(1, \gamma; dt)|_{D_3(\rho_0)} \quad (6.3)$$

for $D_3(\rho_0) = \rho_0^{1-\alpha-2\beta} D_3$ and D_2 unchanged, see (4.3). When $\rho_0 \rightarrow \infty$ in domains A and B and $\rho_0 \rightarrow 0$ in domain C then $D_3(\rho_0) \rightarrow 0$ so that we fall into the situation considered in the scenario (6.2). The latter becomes then the assertion that

$$\mathcal{Q}(\rho_0, \gamma\rho_0; d(\rho_0^{1-\alpha}t)) 1_{\{t < \tau'(\rho_0)\}} \xrightarrow{\rho_0 \rightarrow \infty} \mathcal{Q}^{\text{fr}}(1, \gamma; dt) \quad (6.4)$$

$$\mathcal{Q}(\rho_0, \gamma\rho_0; d(D_3^{-1}\rho_0^{2\beta}s)) 1_{\{s \geq D_3(\rho_0)\tau'(\rho_0)\}} \xrightarrow{\rho_0 \rightarrow \infty} \mathcal{Q}^\infty(\gamma; ds)$$

for $\tau'(\rho_0) = \mathcal{O}(|\ln \rho_0|^\alpha)$.

One of the consequences of such a limiting behavior would be a bifractal scaling with $\rho_0 \rightarrow \infty$ or $\rho_0 \rightarrow 0$ of the moments of the exit time. Indeed,

$$\int_0^\infty t^n \mathcal{Q}(\rho_0, \gamma\rho_0; dt) = \rho_0^{(1-\alpha)n} \int_0^{\tau'(\rho_0)} t^n \mathcal{Q}(\rho_0, \gamma\rho_0; d(\rho_0^{1-\alpha}t)) \\ + D_3^{-n} \rho_0^{2\beta n} \int_{D_3(\rho_0)\tau'(\rho_0)}^\infty s^n \mathcal{Q}(\rho_0, \gamma\rho_0; d(D_3^{-1}\rho_0^{2\beta}s)). \quad (6.5)$$

In the regime of extreme values of ρ_0 , the first term on the right hand side behaves like $\rho_0^{(1-\alpha)n} \int_0^\infty t^n \mathcal{Q}^{\text{fr}}(1, \gamma; dt)$ if we assume (6.4) with a sufficiently strong convergence. Similarly the second term would behave like $D_3^{-n} \rho_0^{2\beta n} \int_{D_3(\rho_0)\tau'(\rho_0)}^\infty s^n \mathcal{Q}^\infty(\gamma; ds)$. If the density of $\mathcal{Q}^\infty(\gamma; ds)$ is integrable at zero, the first term dominates for negative n and the second one for positive n when it behaves as $\mathcal{O}(\rho_0^{2\beta n})$. The “minimal” scenario (6.2) would then imply that

$$\langle t^n \rangle = \begin{cases} \mathcal{O}(\rho_0^{n(1-\alpha)}) & \text{for } n \leq 0, \\ \mathcal{O}(\rho_0^{2\beta n}) & \text{for } n \geq 0 \end{cases} \quad (6.6)$$

for large ρ_0 in domains A and B and for small ρ_0 in domain C. Such a bifractal behavior is, of course, consistent with the earlier conjecture (4.14). The missing mass in the frozen case would be given by $\int_0^\infty \mathcal{Q}^\infty(\gamma; ds)$. Even in the presence of an intermediate regime in the exit time distribution, the scaling (6.6) should set in for $|n| \gg 1$. The convexity (concavity) of the large (small) ρ_0 exponent as a function of n , together with its vanishing at $n = 0$, would then impose the behavior (6.6) for all n .

We have tested the scenario (6.2) numerically. The one-dimensional velocity field with temporal correlations was obtained again using the

Fourier method. Each Fourier mode $v_k(t)$ was generated by integrating the corresponding Ornstein–Uhlenbeck differential equation:

$$dv_k(t) = -\frac{v_k(t)}{\tau(k)} dt + \left(\frac{2E(k)}{\tau(k)}\right)^{1/2} dw_k(t), \quad (6.7)$$

where $\tau(k)$ scales as $k^{-2\beta}$, the energy spectrum of the field is $E(k) \propto k^{-1-2\alpha}$ and $dw_k(t)$ is a standard Brownian motion. The stochastic differential equations (6.7) were integrated by using a simple Euler scheme of order $\frac{1}{2}$.⁽²⁶⁾ The parameters of the flow were $\alpha = 0.75$ and $\beta = 0.3$. The exit times for six different initial separations were measured. The density functions $Q(\rho_0, 1.05\rho_0; t)$ of their distributions are shown in Fig. 6. According to (6.4), by plotting $\rho_0^{1-\alpha} Q$ versus $\rho_0^{\alpha-1} t$ all the curves should collapse at small exit times, as confirmed in Fig. 7. Furthermore, the prediction (6.4) at large exit times is verified in Fig. 8 by collapsing the long-time parts of the curves by plotting $\rho_0^{2\beta} Q$ versus $\rho_0^{-2\beta} t$. Note that the curves for the two smallest values of ρ_0 are not collapsing, in agreement with the previous arguments predicting that the asymptotic behavior sets in at large ρ_0 's. The simulations are consistent with the absence of an intermediate regime but do not really allow to exclude such a possibility.

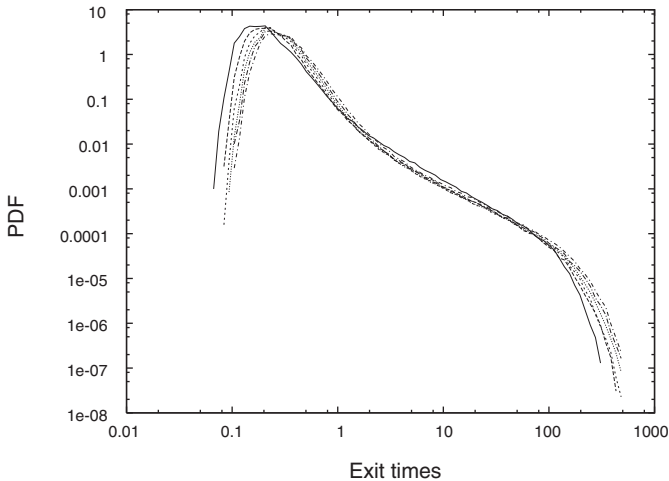


Fig. 6. The density function Q of the exit times for the flow with $\alpha = 0.75$, $\beta = 0.3$, and $\gamma = 1.05$ at six initial separations $\rho_0 = 400, 800, 1200, 1500, 1800, 2100$. The resolution is 32768.

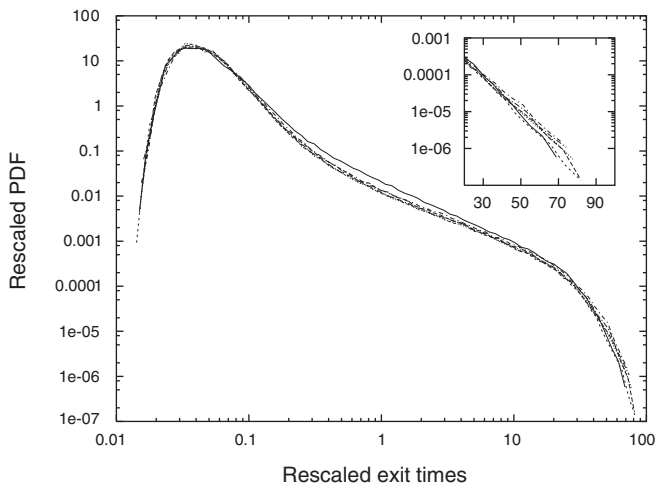


Fig. 7. The same density function as in the previous figure but plotted now as $\rho_0^{1-\alpha} Q$ vs. $\rho_0^{\alpha-1} t$ to display the collapse at small exit times.

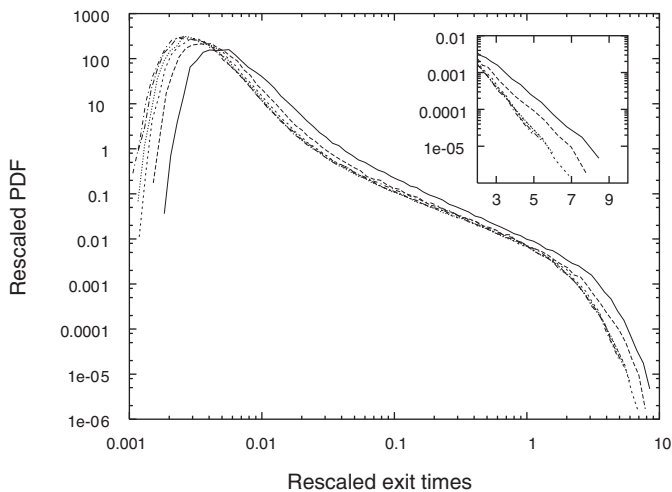


Fig. 8. The same density function as in the previous figure but plotted now as $\rho_0^{2\beta} Q$ vs. $\rho_0^{-2\beta} t$ to display the collapse at large exit times.

7. EULERIAN GAUSSIAN VELOCITIES: SWEEPING EFFECTS

Let us discuss how the Lagrangian flow changes if the Gaussian velocity ensemble 3.1 is used to model the Eulerian velocities rather than the quasi-Lagrangian ones. As already mentioned, the main difference is that, unlike for the Kraichnan model, the separation of two trajectories is not any more a function of velocity differences only and it is strongly influenced by large-scale eddies or the so called sweeping. This effect grows with growing integral scale L and we shall attempt to study its large L asymptotics. It seems to be stronger for small values of β , i.e., for velocities that are almost frozen at small distances.

The r.m.s. value of velocity in the ensemble (3.1) is proportional to L^α , i.e., it becomes large for large L . On the other hand, the r.m.s. equal-time velocity differences on scales much smaller than L are of the order $distance^\alpha$. In particular, on the scales $\sim L^\alpha$ they are of the order $L^{\alpha^2} \ll L^\alpha$. Rewriting the trajectory equation (1.1) as⁷

$$\mathbf{R}(t) = \int_0^t \mathbf{v}(s, \mathbf{0}) ds + \int_0^t [\mathbf{v}(s, \mathbf{R}(s)) - \mathbf{v}(s, \mathbf{0})] ds, \quad (7.1)$$

we may expect that, for fixed t , the first integral is of the order L^α and the second of the order $L^{\alpha^2} \ll L^\alpha$. For bounded times, the first integral should then give the contribution of order L^α to the solution and the second one, with $\mathbf{R}(s)$ replaced by the approximation $\sim L^\alpha$, the term of the order L^{α^2} . More precisely, let us observe that the Gaussian process with the components $L^{-\alpha} \mathbf{v}(t, \mathbf{0})$ and $L^{-\alpha^2} [\mathbf{v}(t, L^\alpha \mathbf{r}) - \mathbf{v}(t, \mathbf{0})]$ converges in law when $L \rightarrow \infty$ to the t -independent Gaussian process $(\mathbf{v}_0, \mathbf{w}(\mathbf{r}))$ with the 2-point functions

$$\begin{aligned} \langle \mathbf{v}_0 \mathbf{v}_0 \rangle &= D_2 \int \frac{1}{k_1^{d+2\alpha}} \frac{d\mathbf{k}}{(2\pi)^d}, \\ \langle \mathbf{w}(\mathbf{r}) \mathbf{w}(\mathbf{r}') \rangle &= D_2 \int \frac{(1 - e^{i\mathbf{k} \cdot \mathbf{r}})(1 - e^{-i\mathbf{k} \cdot \mathbf{r}'})}{k^{d+2\alpha}} \frac{d\mathbf{k}}{(2\pi)^d}, \\ \langle \mathbf{v}_0 \mathbf{w}(\mathbf{r}) \rangle &= 0. \end{aligned} \quad (7.2)$$

Note the independence of \mathbf{v}_0 and $\mathbf{w}(\mathbf{r})$. It is then natural to conjecture that the following convergence in law takes place:

⁷ In principle, we should add the noise to the trajectory but it does not play any role on the scales that will be discussed.

$$L^{-\alpha} \mathbf{R}(t) \xrightarrow{L \rightarrow \infty} \mathbf{v}_0 t, \quad (7.3)$$

$$L^{-\alpha^2} \left[\mathbf{R}(t) - \int_0^t \mathbf{v}(s, \mathbf{0}) ds \right] \xrightarrow{L \rightarrow \infty} \int_0^t \mathbf{w}(\mathbf{v}_0 s) ds. \quad (7.4)$$

In the frozen case or if $\alpha \leq \beta$ or $\alpha > \beta > \alpha(1-\alpha)$, the limits describe the leading terms in the single trajectory statistics for large L . For $\beta \leq \alpha(1-\alpha)$, one should also take into account the term coming from $\int_0^t [\mathbf{v}(s, \mathbf{0}) - \mathbf{v}(0, \mathbf{0})] ds$ which is of order $L^{\alpha-\beta}$. The dominant term of order L^α in $\mathbf{R}(t)$ describes the ballistic motion with the random velocity of the largest scale eddies that sweep the Lagrangian particle along. In Appendix E we prove convergence (7.3) in the frozen one-dimensional model with $\alpha = \frac{1}{2}$.

How does the presence of large scale L in Eulerian velocities influence the Lagrangian particle separation? Let us try to understand this in the one-dimensional frozen model. We shall consider two particle trajectories $x(t)$ and $x(t) + \rho(t)$ starting at time zero at zero and $\rho_0 > 0$, respectively, and we shall try to estimate the behavior of their separation $\rho(t)$. First notice that $\rho(t) \geq 0$, i.e., the order of the particles on the line will never change. For large L , the dominant events are when the velocities of the particles and at the points between them are all of the order L^α and of the same sign during the time interval $(0, t)$. Let us suppose that they are positive, see Fig. 9 (the case of negative velocities can be treated in a symmetric way).

The crucial fact resulting from the one-dimensional geometry where the particle order is preserved by the flow is the magic identity

$$\int_0^{\rho_0} \frac{d\rho}{v(\rho)} = \int_{x(t)}^{x(t)+\rho(t)} \frac{d\rho}{v(\rho)}. \quad (7.5)$$

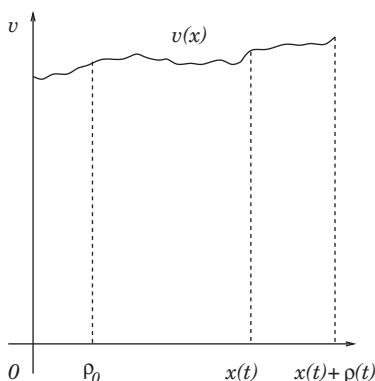


Fig. 9. Positions of two right-moving particles in 1d frozen velocity.

The left hand side is the time Δt that the first particle starting at time zero at $\rho = 0$ takes to reach the initial position ρ_0 of the second one. The right hand side is the time that the second particle takes to go from the time t position $x(t)$ of the first particle (at which it arrives earlier) to its own time t position $x(t) + \rho(t)$. The best way to understand that the above times are equal is by releasing the second particle after the delay Δt so that both particles move subsequently together. The delay changes nothing in the movement of the second particle since the velocity field is frozen. The delayed particle will then be at position $x(t)$ at time t (together with the first particle) and at position $x(t) + \rho(t)$ at time $t + \Delta t$, which shows that it takes time Δt to travel from $x(t)$ to $x(t) + \rho(t)$. Identity (7.5) may be also established more formally by noticing that the time derivative of its right hand side vanishes. Writing for large L

$$x(t) = L^\alpha v_0 t + \mathcal{O}(L^\alpha), \quad v(x(t)) = L^\alpha v_0 + L^{\alpha^2} w(v_0 t) + \mathcal{O}(L^{\alpha^3}), \quad (7.6)$$

see relations (7.3) and (7.4), and anticipating that $\rho(t) = \mathcal{O}(1)$, Eq. (7.5) may be approximated as

$$\frac{\rho_0}{L^\alpha v_0} = \frac{\rho(t)}{L^\alpha v_0 + L^{\alpha^2} w(v_0 t)} + \mathcal{O}(L^{\alpha^3 - 2\alpha}) \quad (7.7)$$

from which we infer that

$$\rho(t) - \rho_0 = L^{\alpha^2 - \alpha} \rho_0 v_0^{-1} w(v_0 t) + \mathcal{O}(L^{\alpha^3 - \alpha}). \quad (7.8)$$

The process $w(x)$ is the fBm with the 2-point function (5.26) (up to normalization). The precise conjecture would then assert the convergence in law

$$L^{\alpha(1-\alpha)} [\rho(t) - \rho_0] \xrightarrow{L \rightarrow \infty} \rho_0 v_0^{\alpha-1} w(t). \quad (7.9)$$

Note that the above calculations indicate that not only a single particle motion, but also the separation of trajectories in the Eulerian frozen one-dimensional velocity ensemble are dominated by the scale L velocities, i.e., by the large eddy sweeping. The effect on the pair dispersion is, however, inverse to that on the single particle motion. Whereas the latter one becomes very fast for large L , the trajectory separation becomes essentially frozen to the initial value in a localization-type effect. It would be interesting to know if such localizing tendency persists in the more general Eulerian Gaussian ensembles (3.1).

That the sweeping modifies the pair separation statistics for finite L may be seen in the following way. There is a competition between two

types of contributions to the dynamics of the pair dispersion $\rho(t)$. The first comes from the configurations where the velocity differences at distances of order $\rho(t)$ are much smaller than the velocity of each particle. The second one from the opposite regime. The two contributions may be separated if we fix the initial velocity $v(0)$ of the first particle, with $v(0) < D_2^{1/2} \rho_0^\alpha$ corresponding to the first regime and $v(0) > D_2^{1/2} \rho_0^\alpha$ to the second one. Denote by $\mathcal{Q}(\rho_0, \rho_1; dt | v(0))$ the conditional distribution of the exit times for fixed $v(0)$. In particular, $\mathcal{Q}(\rho_0, \rho_1; dt | 0)$ is the quasi-Lagrangian distribution studied in the $L \rightarrow \infty$ limit in the previous section. As long as $\rho_0, \rho_1 \ll L$ and $v(0) \ll D_2^{1/2} L^\alpha$, the conditional distribution should be approximately L -independent and, consequently, it should satisfy the scaling identity

$$\mathcal{Q}(\mu^\sigma \rho_0, \mu^\sigma \rho_1; d(\mu t) | \mu^{\sigma-1} v(0)) \simeq \mathcal{Q}(\rho_0, \rho_1; dt | v(0)) \tag{7.10}$$

for $\sigma = \frac{1}{1-\alpha}$. We infer that

$$\mathcal{Q}(\rho_0, \rho_1; dt | v(0)) \simeq \mathcal{Q}(1, \gamma; d(\rho_0^{\alpha-1} t) | \rho_0^{-\alpha} v(0)). \tag{7.11}$$

where, as usually, $\gamma = \frac{\rho_1}{\rho_0}$. Deep in the regime $v(0) < D_2^{1/2} \rho_0^\alpha$ the distribution $\mathcal{Q}(\rho_0, \rho_1; dt | v(0))$ is then essentially quasi-Lagrangian. As for the opposite regime, we may use the magic formula (7.5) with $\rho(t) = \gamma \rho_0$. Deep in that regime, the fluctuations of $v(\rho)$ in both integrals are small and Eq. (7.5) reduces to the approximate identity

$$v(x(t)) \simeq \gamma v(0) \tag{7.12}$$

from which ρ_0 dropped out and which states that the exit time t is the first time when the velocity on the trajectory of the first particle reaches the value $\gamma v(0)$. In the scaling regime, we obtain then

$$\mathcal{Q}(\rho_0, \rho_1; dt | v(0)) \simeq \mathcal{Q}^{sc}(\gamma; d(v(0)^{1-1/\alpha} t)) \tag{7.13}$$

which is consistent with (7.11) in the crossover region $v(0) = \mathcal{O}(\rho^\alpha)$. Even for $v(0) \gtrsim D_2^{1/2} L^\alpha$ where the scaling breaks, the ρ_0 -independence of $\mathcal{Q}(\rho_0, \rho_1; dt | v(0))$ persist so that the contribution of the region $v(0) > D_2^{1/2} \rho_0^\alpha$ to the moments of exit time is approximately ρ_0 -independent for fixed γ . On the other hand, the contribution of the quasi-Lagrangian regime $v(0) < D_2^{1/2} \rho_0^\alpha$ to the n th-moment is approximately proportional to

$$\int_0^{D_2^{1/2} \rho_0^\alpha} dv(0) \int t^n \mathcal{Q}(\rho_0, \gamma \rho_0; dt | v(0)) \simeq D_2^{1/2} \rho_0^{\alpha+n(1-\alpha)} \int t^n \mathcal{Q}(1, \gamma; dt | 0). \tag{7.14}$$

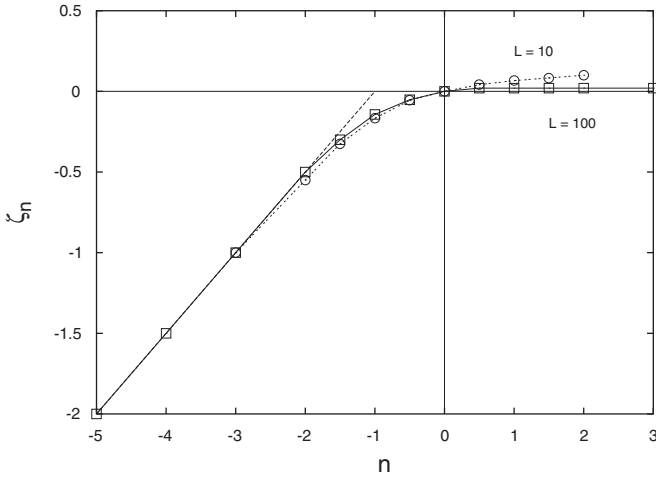


Fig. 10. Scaling exponents of exit-time moments in Eulerian 1d simulations for two different box sizes. Illustration of the sweeping effects.

It dominates for small ρ_0 if $n < -\frac{\alpha}{1-\alpha}$. Altogether, we then expect that in the frozen one-dimensional Eulerian model and for small ρ_0 ,

$$\langle t^n 1_{\{t < \infty\}} \rangle = \mathcal{O}(\rho_0^{\zeta_n}) \quad \text{with} \quad \zeta_n = \begin{cases} \alpha + n(1-\alpha) & \text{for } n \leq -\frac{\alpha}{1-\alpha}, \\ 0 & \text{for } n \geq -\frac{\alpha}{1-\alpha}, \end{cases} \quad (7.15)$$

i.e., again a bifractal situation. The prediction seems to be confirmed, at least for large $|n|$, by numerical simulations, see Fig. 10 where the scaling exponents for two sizes of the periodic box are plotted.

APPENDIX A

We gather here several explicit formulae for the exit time distribution in the Kraichnan model and discuss in more detail some of their properties mentioned in the main text.

For $\zeta = 2$ and $L = \infty$, i.e., in the smooth case with scaling,

$$\begin{aligned} \mathcal{Q}(\rho_0, \rho_1; dt) &= \frac{|\ln(\rho_1/\rho_0)|}{\sqrt{4\pi D_1' t^3}} e^{-\frac{1}{4D_1' t} (\ln(\rho_1/\rho_0) - \lambda t)^2} dt \\ &= \frac{|\ln(\rho_1/\rho_0)|}{\sqrt{4\pi D_1' t^3}} e^{\frac{\lambda \ln(\rho_1/\rho_0)}{2D_1'}} e^{-\frac{1}{4D_1' t} \ln^2(\rho_1/\rho_0) - \frac{\lambda^2}{4D_1'} t} dt, \end{aligned} \quad (A.1)$$

as given by Eq. (2.16) with the use of the explicit expression for the Dirichlet heat kernel

$$e^{-tM_D}(\rho_0, \rho) = \frac{1}{\sqrt{4\pi D'_1 t} \rho} \left(e^{-\frac{1}{4D'_1 t} (\ln(\rho/\rho_0) - \lambda t)^2} - e^{\frac{\lambda}{D'_1} \ln(\rho_1/\rho_0) - \frac{1}{4D'_1 t} (\ln(\rho\rho_0/\rho_1^2) - \lambda t)^2} \right). \tag{A.2}$$

Note the decay $\sim e^{-\frac{1}{4D'_1 t} \ln^2(\rho_1/\rho_0)}$ of the density of $\mathcal{Q}(\rho_0, \rho_1; dt)$ for small t and its exponential tail $\sim e^{-\frac{\lambda^2}{4D'_1 t} t}$ for large t indicating the non-Gaussian character of small and large fluctuations of t . For the conditional moments of the exit time, one obtains:

$$\begin{aligned} \langle t^n \rangle_c &= \frac{|\lambda|}{\sqrt{\pi D'_1}} \left(\frac{|\ln(\rho_1/\rho_0)|}{|\lambda|} \right)^{n+\frac{1}{2}} e^{\frac{|\lambda \ln(\rho_1/\rho_0)|}{2D'_1}} K_{|n+\frac{1}{2}|} \left(\frac{|\lambda \ln(\rho_1/\rho_0)|}{2D'_1} \right) \\ &= \sum_{k=0}^{|n-\frac{1}{2}|-\frac{1}{2}} \frac{(|n-\frac{1}{2}|-\frac{1}{2}+k)!}{k! (|n-\frac{1}{2}|-\frac{1}{2}-k)!} \left(\frac{D'_1}{\lambda^2} \right)^k \left(\frac{|\ln(\rho_1/\rho_0)|}{|\lambda|} \right)^{n-k}, \end{aligned} \tag{A.3}$$

where the first expression with the Bessel function holds for all real n and the second one for integer n . The unconditioned moments diverge for $n > 0$ if $\lambda \ln(\rho_1/\rho_0) < 0$ due to the finite probability of infinite exit times. The conditional characteristic function has the form:

$$\langle e^{i\omega t} \rangle_c = \left(\frac{\rho_1}{\rho_0} \right)^{\pm \frac{\lambda}{D'_1} \left(\frac{1}{2} - \sqrt{\frac{1}{4} - i \frac{D'_1 \omega}{\lambda^2}} \right)}, \tag{A.4}$$

where the square root is taken with the positive real part and the sign is that of $\lambda \ln(\rho_1/\rho_0)$. The decay $\sim e^{-|\ln(\rho_1/\rho_0)| \sqrt{|\omega|/D'_1}}$ at large $|\omega|$ along the positive imaginary axis and the presence of the singularity at $\omega = -i \frac{\lambda^2}{4D'_1}$ reflect the small and large t behavior of the density of $\mathcal{Q}(\rho_0, \rho_1; dt)$.

For $0 < \xi < 2$ and $L = \infty$, i.e., in the non-smooth case with scaling,

$$\begin{aligned} &(M_D - i\omega)^{-1}(\rho_0, \rho) \\ &= \frac{1}{D'_1} \mathcal{W}^{-1} \rho^{a-\xi} f_{\mp}(\rho_1)^{-1} \\ &\quad \begin{cases} f_{\mp}(\rho_0)(f_{\pm}(\rho) f_{\mp}(\rho_1) - f_{\mp}(\rho) f_{\pm}(\rho_1)) & \text{for } \rho_0 \leq \rho, \\ f_{\mp}(\rho)(f_{\pm}(\rho_0) f_{\mp}(\rho_1) - f_{\mp}(\rho_0) f_{\pm}(\rho_1)) & \text{for } \rho_0 \geq \rho \end{cases} \end{aligned} \tag{A.5}$$

on the interval $[0, \rho_1]$ with the upper sign pertaining to the weakly compressible $\wp < \frac{d}{\xi^2}$ region and the lower one to the strongly compressible one

$\wp \geq \frac{d}{\xi^2}$. Functions f_{\pm} are the two independent solutions of the eigenfunction equation $(M - i\omega) f = 0$ expressed by the Bessel functions:

$$f_{\pm}(\rho) = \rho^{\frac{1-a}{2}} J_{\pm b} \left(\frac{2}{2-\xi} \sqrt{\frac{i\omega}{D'_1}} \rho^{2-\xi} \right) \quad (\text{A.6})$$

and

$$\mathcal{W} = \rho^a (f_{\pm}(\rho) \partial_{\rho} f_{\mp}(\rho) - f_{\mp}(\rho) \partial_{\rho} f_{\pm}(\rho)) \quad (\text{A.7})$$

is their ρ -independent Wronskian. The eigenfunction f_+ (f_-) satisfies the singular Dirichlet (Neumann) condition at the origin imposed by the limit when the trajectory noise is turned off for weak (strong) compressibility, see ref. 23. Equation (2.19) implies that

$$\langle e^{i\omega t} 1_{\{t < \infty\}} \rangle = \frac{f_{\mp}(\rho_0)}{f_{\mp}(\rho_1)}. \quad (\text{A.8})$$

For $\omega \rightarrow 0$ the eigenfunction f_- reduces to a constant whereas f_+ becomes proportional to ρ^{1-a} resulting in relation (2.23).

For the conditional characteristic function, one obtains

$$\langle e^{i\omega t} \rangle_c = \left(\frac{\rho_0}{\rho_1} \right)^{\mp \frac{a-1}{2}} \frac{J_{\mp b} \left(\frac{2}{2-\xi} \sqrt{\frac{i\omega}{D'_1}} \rho_0^{2-\xi} \right)}{J_{\mp b} \left(\frac{2}{2-\xi} \sqrt{\frac{i\omega}{D'_1}} \rho_1^{2-\xi} \right)}. \quad (\text{A.9})$$

The moments of the exit times may be derived from this expression by expanding the right hand side in powers of ω . In particular, one obtains for the conditional average of the exit time the result:

$$\langle t \rangle_c = \frac{(\rho_1/\rho_0)^{2-\xi} - 1}{(2-\xi)(2-\xi \mp (1-a)) D'_1} \rho_0^{2-\xi} \quad (\text{A.10})$$

which reproduces in the $\xi \rightarrow 2$ limit the $n = 1$ version of Eq. (A.3). The higher order moments $\langle t^n \rangle_c$ are proportional to $\rho_0^{n(2-\xi)}$ if $\frac{\rho_1}{\rho_0}$ is kept constant. The decay $\propto e^{-\theta(\sqrt{|\omega|})}$ of the absolute value of the right hand side of Eq. (A.9) at large positive or negative ω guarantees that the exit time distribution $\mathcal{Q}(\rho_0, \rho_1; dt)$ has a smooth density. Since the latter is zero for negative t , it must vanish with all derivatives at $t = 0$. More exactly, the decay $\sim e^{-b_1 \sqrt{|\omega|}}$ of the characteristic function (A.9) along the positive imaginary axis of ω , with $b_1 = 2(2-\xi)^{-1} (D'_1)^{-1/2} (\rho_1^{(2-\xi)/2} - \rho_0^{(2-\xi)/2})$,

signals the behavior $\sim e^{-\frac{b_1^2}{4t}}$ of the density of $\mathcal{Q}(\rho_0, \rho_1; dt)$ for small t . The analyticity properties of the right hand side of (A.9) imply the exponential decay $\sim e^{-b_2 t}$ of the density of $\mathcal{Q}(\rho_0, \rho_1; dt)$ for large t , with the rate $b_2 = \frac{1}{4}(2-\xi)^2 D_1' \rho_1^{\xi-2} x_0^2$ where x_0 is the (real) zero of $J_{\mp b}(z)$ closest to the origin. In this respect, the exit time distribution $\mathcal{Q}(\rho_0, \rho_1; dt)$ behaves similarly for weak and for strong compressibility, the main difference between the two cases consisting in the missing mass in the latter case.

For $\rho_1 < \rho_0$, the statistics of the time of exit through ρ_1 is related to the resolvent kernel of the generator M_D on the interval $[\rho_1, \infty)$. For $0 < \xi < 2$, the latter is given by a formula like (A.5) but with the overall minus sign, the cases $\rho_0 \leq \rho$ and $\rho_0 \geq \rho$ interchanged, and the functions f_{\mp} , f_{\pm} replaced by the Hankel functions

$$f^{(i)}(\rho) = \rho^{\frac{1-a}{2}} H_b^{(i)} \left(\frac{2}{2-\xi} \sqrt{\frac{i\omega}{D_1'}} \rho^{2-\xi} \right) \quad (\text{A.11})$$

for $i = 1, 2$, respectively. The square root in the argument of the Hankel functions should be taken with the positive imaginary part so that it is the eigenfunction $f^{(1)}$ which has a stretched exponential decay for large ρ . For the characteristic function of the exit time, Eq. (2.19) gives:

$$\langle e^{i\omega t} 1_{\{t < \infty\}} \rangle = \frac{f^{(1)}(\rho_0)}{f^{(1)}(\rho_1)}. \quad (\text{A.12})$$

When $\omega \rightarrow 0$, the eigenfunction $f^{(1)}$ becomes proportional to ρ^{1-a} if $a > 1$, i.e., if $b < 0$ or $\wp < \frac{d-2}{2\xi} + \frac{1}{2}$ and to a constant if $a \leq 1$, i.e., if $b \geq 0$ or $\wp \geq \frac{d-2}{2\xi} + \frac{1}{2}$, resulting in relation (2.24).

The conditional characteristic function is given by the expression

$$\langle e^{i\omega t} \rangle_c = \left(\frac{\rho_0}{\rho_1} \right)^{\frac{|1-a|}{2}} \frac{H_b^{(1)} \left(\frac{2}{2-\xi} \sqrt{\frac{i\omega}{D_1'}} \rho_0^{2-\xi} \right)}{H_b^{(1)} \left(\frac{2}{2-\xi} \sqrt{\frac{i\omega}{D_1'}} \rho_1^{2-\xi} \right)}. \quad (\text{A.13})$$

Again, its absolute value decays as $e^{-\theta(\sqrt{|\omega|})}$ for large $|\omega|$ implying that $\mathcal{Q}(\rho_0, \rho_1; dt)$ has a smooth density that vanishes with all derivatives at the origin. More exactly, the decay $\sim e^{-b_1 \sqrt{|\omega|}}$ of (A.13) along the positive imaginary axis, where b_1 is as for $\rho_1 > \rho_0$ but with ρ_0 and ρ_1 interchanged, implies again the behavior $\sim e^{-\frac{b_1^2}{4t}}$ of the density of the exit time distribution $\mathcal{Q}(\rho_0, \rho_1; dt)$ for small t . Since $H_b^{(1)}(z)$ is a combination of $z^{\pm b}$ with coefficients that are entire functions of z^2 (for non-integer b), it follows that

$\langle e^{i\omega t} \rangle_c$ has the n th derivative over ω at the origin if (and only if) $n < |b|$. That implies that for $\rho_1 < \rho_0$ the density of $\mathcal{Q}(\rho_0, \rho_1; dt)$ has a power decay for large t , unlike for $\rho_1 > \rho_0$ where it decayed exponentially. This leads to even more non-Gaussian large deviations of the exit time.

APPENDIX B

We shall establish here the estimate (5.9) on the average time, given by Eq. (5.8), that the trajectory takes to reach the first zero of the Brownian motion $w(\rho)$ between ρ_0 and ρ_2 . To this end, let us note that for $\delta > 0$,

$$\begin{aligned} \int_0^\infty e^{-\frac{(w+w_2)^2}{2(\rho_2-\rho)}} \frac{\sqrt{2} dw_2}{\sqrt{\pi(\rho_2-\rho)}} &\leq \sqrt{2} e^{-\frac{w^2}{4(\rho_2-\rho)}} \\ &\leq \sqrt{2} \left(\frac{\rho_2}{\rho_2-\rho} \right)^\delta e^{-\frac{w^2}{4(\rho_2-\rho)}} \\ &\leq \sqrt{2} (4\delta)^\delta e^{-\delta} \frac{\rho_2^\delta}{w^{2\delta}}, \end{aligned} \quad (\text{B.1})$$

where the last inequality follows from $xe^{-x} \leq e^{-1}$. Employing the bound (B.1) for $0 < \delta < 1/2$ and extending the integral over ρ in (5.8) to infinity with the use of the identity

$$\int_{\rho_0}^\infty \left(e^{-\frac{(w_0-w)^2}{2(\rho-\rho_0)}} - e^{-\frac{(w_0+w)^2}{2(\rho-\rho_0)}} \right) \frac{d\rho}{\sqrt{2\pi(\rho-\rho_0)}} = w_0 + w - |w_0 - w|, \quad (\text{B.2})$$

we obtain

$$\begin{aligned} &\langle t_+ 1_{\{w(\rho_0) > 0, \rho_+ \leq \rho_2\}} \rangle \\ &\leq \sqrt{2} (4\delta)^\delta e^{-\delta} \rho_2^\delta \int_0^\infty e^{-\frac{w_0^2}{2\rho_0}} \frac{dw_0}{\sqrt{2\pi\rho_0}} \int_0^\infty \frac{(w_0 + w - |w_0 - w|) dw}{w^{1+2\delta}} \\ &= \frac{(2\delta)^\delta e^{-\delta} \Gamma(1-\delta)}{\sqrt{\pi} \delta(1-2\delta)} \rho_0^{1/2-\delta} \rho_2^\delta. \end{aligned} \quad (\text{B.3})$$

The minimization over δ gives the inequality (5.9).

APPENDIX C

The constraint moments of the exit time (5.12) in the frozen one-dimensional model with $\alpha = \frac{1}{2}$ and $L = \infty$ take the form

$$\begin{aligned}
 \langle t^n \mathbf{1}_{\{t < \infty\}} \rangle &= n! \int_{\rho_0 \leq \rho' \leq \dots \leq \rho^{(n)} \leq \rho_1} d\rho' \dots d\rho^{(n)} \int_0^\infty e^{-\frac{w_0^2}{2\rho_0}} \frac{dw_0}{\sqrt{2\pi\rho_0}} \\
 &\cdot \prod_{i=1}^n \int_0^\infty \left(e^{\frac{-(w^{(i-1)} - w^{(i)})^2}{2(\rho^{(i)} - \rho^{(i-1)})}} - e^{\frac{-(w^{(i-1)} + w^{(i)})^2}{2(\rho^{(i)} - \rho^{(i-1)})}} \right) \frac{dw^{(i)}}{\sqrt{2\pi(\rho^{(i)} - \rho^{(i-1)})} w^{(i)}} \\
 &\cdot \int_0^\infty \left(e^{\frac{-(w^{(n)} - w_1)^2}{2(\rho_1 - \rho^{(n)})}} - e^{\frac{-(w^{(n)} + w_1)^2}{2(\rho_1 - \rho^{(n)})}} \right) \frac{dw_1}{\sqrt{2\pi(\rho_1 - \rho^{(n)})}} \quad (C.1)
 \end{aligned}$$

with $\rho^{(0)} \equiv \rho_0$ and $w^{(0)} \equiv w_0$. It is easy to show that the expression on the right hand side is finite. Indeed, bounding the last integral by $\sqrt{\frac{2}{\pi(\rho_1 - \rho^{(n)})}} w^{(n)}$ as in estimating (5.10) and proceeding further the same way, we obtain the inequality

$$\begin{aligned}
 \langle t^n \mathbf{1}_{\{t < \infty\}} \rangle &\leq \frac{1}{\pi} \left(\frac{2}{\pi} \right)^{n/2} \sqrt{\rho_0} n! \int_{\rho_0 \leq \rho' \leq \dots \leq \rho^{(n)} \leq \rho_1} \frac{d\rho' \dots d\rho^{(n)}}{\sqrt{(\rho' - \rho_0) \dots (\rho_1 - \rho^{(n)})}} \\
 &\leq \frac{2^n}{\sqrt{2\pi}} \frac{n!}{(n-1)!!} \left(\frac{\rho_1}{\rho_0} - 1 \right)^{\frac{n-1}{2}} \rho_0^{\frac{n}{2}}, \quad (C.2)
 \end{aligned}$$

where the last line results from the inductive calculation of the $\rho^{(i)}$ integrals.

APPENDIX D

This appendix is devoted to the spectral analysis of the operator \mathcal{K}_- given by Eq. (5.19) and pertaining to the long-time behavior of the $d = 1$, $\alpha = \frac{1}{2}$ exit times. The two eigen-solutions of \mathcal{K}_- corresponding to an eigenvalue λ may be expressed by the Whittaker functions

$$\psi_\lambda(w) = M \frac{1}{\sqrt{-2\lambda}} \frac{1}{2} (2 \sqrt{-2\lambda} w), \quad \varphi_\lambda(w) = W \frac{1}{\sqrt{-2\lambda}} \frac{1}{2} (2 \sqrt{-2\lambda} w). \quad (D.1)$$

The spectrum of \mathcal{K}_- on the positive half-line and with the Dirichlet boundary condition at the origin is composed of the half-line $[0, \infty)$ (continuous spectrum) and of discrete negative eigenvalues $E_n = -\frac{1}{2n^2}$ for $n = 1, 2, \dots$ corresponding to the bound states in the attractive potential. The eigenfunctions in the spectrum are $\psi_E(w)$ where in (D.1) for $E > 0$ we choose the square root with positive imaginary part and for $E = E_n$ the positive one. These functions vanish at zero. They are imaginary and

oscillating at infinity for $E > 0$. For $E = E_n$, they are real and decaying exponentially. In the latter case, the two eigen-solutions (D.1) become proportional and may be expressed by the Laguerre polynomials, similarly as for the three-dimensional Schrödinger operator in the attractive Coulomb potential:

$$\begin{aligned} M_{n, \frac{1}{2}}\left(\frac{2}{n}w\right) &= \frac{(-1)^{n-1}}{n!} W_{n, \frac{1}{2}}\left(\frac{2}{n}w\right) \\ &= \frac{2}{n^2} w e^{-\frac{1}{n}w} L_{n-1}^1\left(\frac{2}{n}w\right) = \frac{1}{n!} e^{z/2} \frac{d^{n-1}}{dz^{n-1}} (z^n e^{-z})|_{z=\frac{2}{n}w}. \end{aligned} \quad (\text{D.2})$$

The resolvent kernel of \mathcal{K}_- takes the form

$$(\mathcal{K}_- - \lambda)^{-1}(w_0, w_1) = \frac{2}{\mathcal{W}} \begin{cases} \psi_\lambda(w_0) \varphi_\lambda(w_1) & \text{for } w_0 \leq w_1, \\ \varphi_\lambda(w_0) \psi_\lambda(w_1) & \text{for } w_0 \geq w_1, \end{cases} \quad (\text{D.3})$$

with the Wronskian

$$\mathcal{W} = \varphi_\lambda(w) \partial_w \psi_\lambda(w) - \psi_\lambda(w) \partial_w \varphi_\lambda(w) = 2 \sqrt{-2\lambda} / \Gamma(1 - \frac{1}{\sqrt{-2\lambda}}), \quad (\text{D.4})$$

where in the expression for the resolvent the square roots are taken positive for λ sufficiently negative and continued analytically to the other values of λ outside the spectrum. The discrete eigenvalues E_n appear as poles in the right hand side of (D.3) with the residue

$$-\sqrt{-2E_n} \psi_{E_n}(w_0) \overline{\psi_{E_n}(w_1)} \quad (\text{D.5})$$

originating in the zeros of the Wronskian. Along the positive axis of λ , the right hand side of (D.3) has a cut

$$\frac{\pi i}{E} (1 - e^{-\frac{2\pi}{\sqrt{2E}}})^{-1} \psi_E(w_0) \overline{\psi_E(w_1)}. \quad (\text{D.6})$$

It follows that the spectral density of \mathcal{K}_- has the form

$$\nu(E) = \sum_{n=1}^{\infty} \sqrt{-2E_n} \delta(E - E_n) + \frac{1}{2E} (1 - e^{-\frac{2\pi}{\sqrt{2E}}})^{-1} \quad (\text{D.7})$$

and that

$$\begin{aligned} & \int_0^\infty e^{-|\omega|^2 (\rho_1 - \rho_0) \mathcal{K}_-} (w_0, w_1) dw_1 \\ &= \sum_{n=1}^\infty e^{\frac{|\omega|^2 (\rho_1 - \rho_0)}{2n^2}} \frac{1}{n} M_{n, \frac{1}{2}} \left(\frac{2}{n} w_0 \right) \int_0^\infty M_{n, \frac{1}{2}} \left(\frac{2}{n} w_1 \right) dw_1 \\ & \quad - \int_0^\infty dw_1 \int_0^\infty \frac{e^{-|\omega|^2 (\rho_1 - \rho_0) E}}{2E(1 - e^{-\frac{2\pi}{\sqrt{2E}}})} M_{\frac{1}{i\sqrt{2E}}, \frac{1}{2}}(2i \sqrt{2E} w_0) M_{\frac{1}{i\sqrt{2E}}, \frac{1}{2}}(2i \sqrt{2E} w_1) dE. \end{aligned} \tag{D.8}$$

Substituting this expression to Eq. (5.18), one can see that the contribution of the ground state of \mathcal{K}_- dominates for $\omega = -i |\omega|$ and large $|\omega|$ so that

$$\langle e^{i\omega t} 1_{\{t < \infty\}} \rangle = \frac{2\sqrt{2}}{\sqrt{\pi\rho_0} |\omega|} e^{\frac{|\omega|^2 (\rho_1 - \rho_0)}{2}} (1 + \mathcal{O}(|\omega|^{-2})). \tag{D.9}$$

APPENDIX E

As an illustration to Section 7, we shall prove here the convergence (7.3) for the one-dimensional frozen case of the Gaussian ensemble (3.1) of Eulerian velocities with $\alpha = \frac{1}{2}$. Using the scaling properties of the frozen velocities, both $x(t)$ and v_0 may be realized on the same probability space corresponding to the velocity process $\tilde{v}(x)$ with $L = 1$. This is done by setting

$$x(t) = L\tilde{x}(L^{-\frac{1}{2}}t), \quad v_0 = \tilde{v}(0), \tag{E.1}$$

where $\tilde{x}(t)$ is the Lagrangian trajectory in the field $\tilde{v}(x)$ such that $\tilde{x}(0) = 0$. We shall prove the (stronger) convergence (3.1) in the L^2 -norm on the probability space of \tilde{v} :

$$\langle [L^{\frac{1}{2}}\tilde{x}(L^{-\frac{1}{2}}t) - \tilde{v}(0) t]^2 \rangle \xrightarrow{L \rightarrow \infty} 0. \tag{E.2}$$

If $\tilde{v}(0) > 0$ then $\tilde{x}(t) > 0$ and, symmetrically, if $\tilde{v}(0) < 0$ then $\tilde{x}(t) < 0$. The contributions of the two cases to the expectation (E.2) are equal so let us study the case $\tilde{v}(0) > 0$. It will be more convenient to estimate the expectations of the exit time $\tilde{t}(x)$ of \tilde{x} through $x > 0$ related to $\tilde{x}(t)$ by the identity

$$1_{\{\tilde{x}(t) \geq x\}} = 1_{\{\tilde{t}(x) \leq t\}}. \tag{E.3}$$

Since $\tilde{t}(x) = \int_0^x \frac{dy}{\tilde{v}(y)}$ if $\tilde{v} > 0$ on $[0, x)$ and is infinite otherwise, we have easy bounds

$$1_{\{\tilde{v}_{\min} \geq x/t\}} \leq 1_{\{\tilde{t}(x) \leq t\}} \leq 1_{\{\tilde{v}_{\text{av}} \geq x/t\}} \quad (\text{E.4})$$

with \tilde{v}_{\min} being the minimum of \tilde{v} on the interval $[0, x]$ and $\tilde{v}_{\text{av}} = \frac{1}{x} \int_0^x \tilde{v}$ its average value. Now, with the use of the identity (E.3) and integration by parts, the L^2 -norm on the left hand side of (E.2) may be rewritten as

$$4 \int_0^\infty x \langle 1_{\{\tilde{t}(L^{-\frac{1}{2}x}) \leq L^{-\frac{1}{2}t}\}} \rangle dx - 4t \int_0^\infty \langle 1_{\{\tilde{t}(L^{-\frac{1}{2}x}) \leq L^{-\frac{1}{2}t}\}} \tilde{v}(0) \rangle dx + t^2 \langle \tilde{v}(0)^2 \rangle. \quad (\text{E.5})$$

From the explicit expressions for the Gaussian field expectations, it follows that, for \tilde{v}_{\min} and \tilde{v}_{av} standing now for the minimum and the mean of \tilde{v} on the interval $[0, L^{-\frac{1}{2}x}]$,

$$\lim_{L \rightarrow \infty} \langle 1_{\{\tilde{v}_{\min} \geq x/t\}} \rangle = \lim_{L \rightarrow \infty} \langle 1_{\{\tilde{v}_{\text{av}} \geq x/t\}} \rangle = \langle 1_{\{\tilde{v}(0) > x/t\}} \rangle, \quad (\text{E.6})$$

so that also

$$\lim_{L \rightarrow \infty} \langle 1_{\{\tilde{t}(L^{-\frac{1}{2}x}) \leq L^{-\frac{1}{2}t}\}} \rangle = \langle 1_{\{\tilde{v}(0) > x/t\}} \rangle \quad (\text{E.7})$$

and similarly with the insertion of $\tilde{v}(0)$. It is also easy to show a uniform in L bound $\langle 1_{\{\tilde{v}_{\min} \geq x/t\}} \rangle \leq e^{-C(x/t)^2}$. From the Dominated Convergence Theorem, the limit of (E.5) is then equal to the expression

$$4 \int_0^\infty x \langle 1_{\{\tilde{v}(0) \geq x/t\}} \rangle dx - 4t \int_0^\infty \langle 1_{\{\tilde{v}(0) \geq x/t\}} \tilde{v}(0) \rangle dx + t^2 \langle \tilde{v}(0)^2 \rangle \quad (\text{E.8})$$

which vanishes in a Gaussian ensemble. Generalization of this proof to the case with $\alpha \neq 0$ does not pose much problem.

ACKNOWLEDGMENTS

The work of MC was supported by the Fundação para a Ciência e a Tecnologia Grant: PRAXIS XXI/BD/21413/99. K.G., P.H., A.K., and M.V. are grateful to the Erwin Schrödinger Institute in Vienna and the Institute for Advanced Study in Princeton where parts of the work on the paper were done. K.G. acknowledges the support of the von Neumann Fund and M.V. the Ralph E. and Doris M. Hansmann Membership at the

IAS. A.K. and M.V. were also supported by the European Union under the Contracts FMRX-CT98-0175 and HPRN-CT-2000-00162, respectively.

REFERENCES

1. D. J. Amit, *Field Theory, the Renormalization Group, and Critical Phenomena* (World Scientific, Singapore, 1984).
2. N. V. Antonov, Anomalous scaling regimes of a passive scalar advected by the synthetic velocity field, *Phys. Rev. E* **60**:6691–6707 (1999).
3. M. Avellaneda and A. J. Majda, Mathematical models with exact renormalization for turbulent transport, *Commun. Math. Phys.* **133**:381–429 (1990).
4. M. Avellaneda and A. J. Majda, Mathematical models with exact renormalization for turbulent transport, II: Fractal interphases, non-Gaussian statistics, and sweeping effects, *Commun. Math. Phys.* **146**:139–204 (1992).
5. D. Bernard, K. Gawędzki, and A. Kupiainen, Slow modes in passive advection, *J. Stat. Phys.* **90**:519–569 (1998).
6. G. Boffetta, A. Celani, A. Crisanti, and A. Vulpiani, Pair dispersion in synthetic fully developed turbulence, *Phys. Rev. E* **60**:6734–6741 (1999).
7. A. Borodin and P. Salminen, *Handbook of Brownian Motion: Facts and Formulae* (Birkhäuser, Boston, 1996).
8. L. Breiman, *Probability* (Addison–Wesley, Reading, MA, 1968).
9. M. Chertkov, G. Falkovich, I. Kolokolov, and V. Lebedev, Statistics of a passive scalar advected by a large-scale 2D velocity field: Analytic solution, *Phys. Rev. E* **51**:5609–5627 (1995).
10. M. Chertkov, G. Falkovich, and V. Lebedev, Nonuniversality of the scaling exponents of a passive scalar convected by a random flow, *Phys. Rev. Lett.* **76**:3707–3710 (1996).
11. M. Chertkov, I. Kolokolov, and M. Vergassola, Inverse versus direct cascades in turbulent advection, *Phys. Rev. Lett.* **80**:512–515 (1998).
12. W. E and E. Vanden Eijnden, Generalized flows, intrinsic stochasticity, and turbulent transport, *Proc. Natl. Acad. Sci. USA* **97**:8200–8205 (2000).
13. W. E and E. Vanden Eijnden, Turbulent Prandtl number effect on passive scalar advection, *Physica D* **152–153**:636–645 (2001).
14. G. Falkovich, K. Gawędzki, and M. Vergassola, Particles and fields in fluid turbulence, *Rev. Modern Phys.* **73**:913–975 (2001).
15. A. Fannjiang, Phase diagram for turbulent transport: Sampling drift, eddy diffusivity, and variational principles, *Physica D* **136**:145–174 (2000). Erratum: *Physica D* **157**:166–168 (2001).
16. A. Fannjiang, Richardson’s laws for relative dispersion in colored-noise flows with Kolmogorov-type spectra, arXiv:math-ph/0209007.
17. A. Fannjiang, Convergence of passive scalars in Ornstein–Uhlenbeck flows to Kraichnan’s model, arXiv:math-ph/0209011.
18. A. Fannjiang, T. Komorowski, and S. Peszat, Lagrangian dynamics for a passive tracer in a class of Gaussian Markovian flows, *Stochastic Process. Appl.* **97**:171–198 (2002).
19. W. Feller, The parabolic differential equations and the associated semi-groups of transformations, *Ann. Math.* **55**:468–519 (1952).
20. U. Frisch, A. Mazzino, and M. Vergassola, Intermittency in passive scalar advection, *Phys. Rev. Lett.* **80**:5532–5535 (1998).
21. O. Gat and R. Zeitak, Multiscaling in passive scalar advection as stochastic shape dynamics, *Phys. Rev.* **57**:5511–5519.

22. K. Gawędzki, Turbulent advection and breakdown of the Lagrangian flow, in *Intermittency in Turbulent Flows*, J. C. Vassilicos, ed. (Cambridge University Press, Cambridge, 2001), pp. 86–104.
23. K. Gawędzki and P. Horvai, Sticky behavior of fluid particles in the compressible Kraichnan model, arXiv:nlin.CD/0309027.
24. P. Horvai, Sticky behavior of fluid particles in the Kraichnan model with intermediate compressibility, in preparation.
25. P. Horvai, T. Komorowski, and J. Wehr, in preparation.
26. P. E. Kloeden and E. Platen, *Numerical Solution of Stochastic Differential Equations* (Springer, Berlin, 1992).
27. R. H. Kraichnan, Small-scale structure of a scalar field convected by turbulence, *Phys. Fluids* **11**:945–963 (1968).
28. Y. Le Jan and O. Raimond, Integration of Brownian vector fields, *Ann. Probab.* **30**: 826–873 (2002).
29. Y. Le Jan and O. Raimond, Flows, coalescence and noise, arXiv:math.PR/0203221.
30. A. J. Majda and P. R. Kramer, Simplified models for turbulent diffusion: Theory, numerical modelling, and physical phenomena, *Phys. Rep.* **314**:237–574 (1999).
31. G. M. Molchan, Maximum of a fractional Brownian motion: Probabilities of small values, *Commun. Math. Phys.* **205**:97–111 (1999).
32. L. Onsager, Statistical hydrodynamics, *Nuovo Cimento Suppl.* **2** 6:279–287 (1949).
33. L. F. Richardson, Atmospheric diffusion shown on a distance-neighbour graph, *Proc. Roy. Soc. London Ser. A* **110**:709–737 (1926).
34. E. Vanden Eijnden, Statistical description of turbulence. Application to anomalous transport in plasmas, Ph.D. thesis, Université Libre de Bruxelles (1997).